A test of leading-twist/leading-order approach with high statistical precision DVCS data

M. Defurne

CEA Saclay - IRFU/SPhN

November 10^{th} 2016

Nucleon structure and distributions

TMDs: Fraction of longitudinal momentum x et transverse momentum k

GPDs: Fraction of longitudinal momentum x et transverse position b

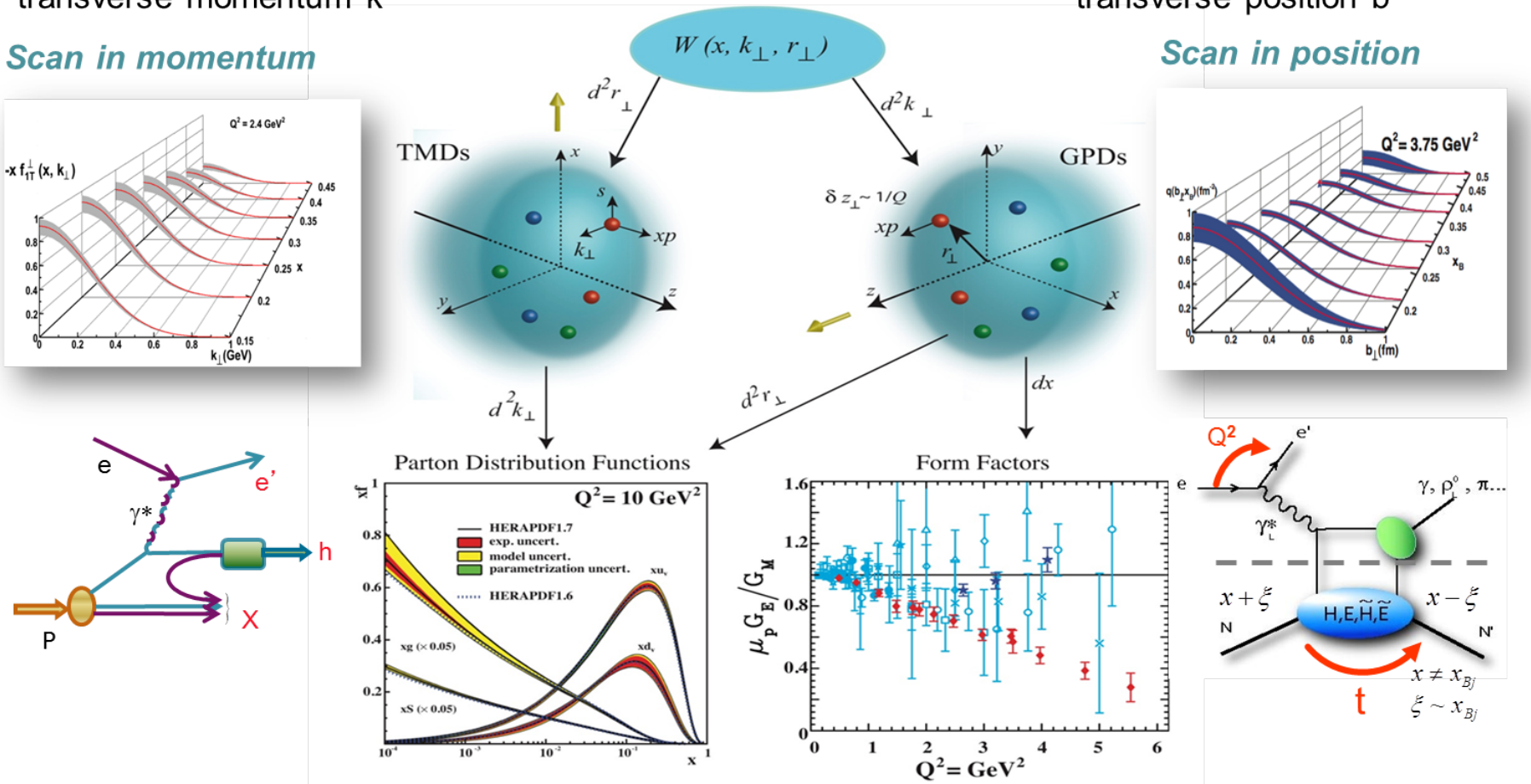

DVCS and GPDs

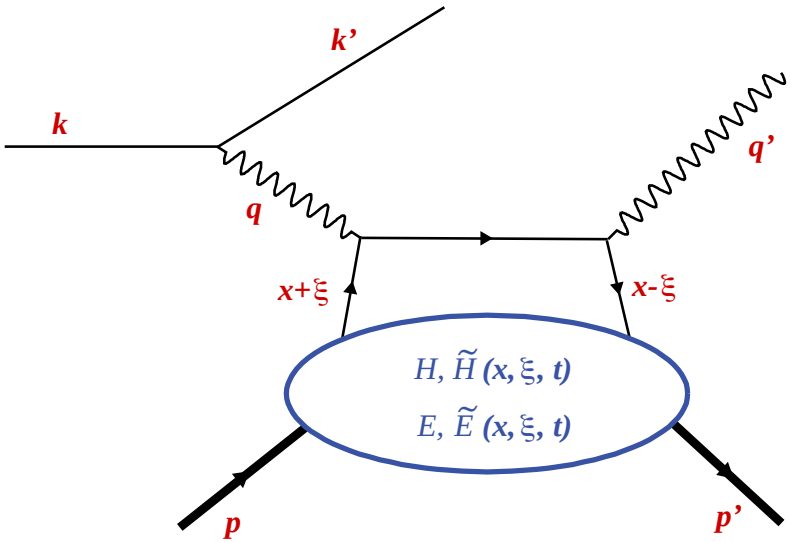

- $Q^2 = -q^2 = -(k - k')^2$.
- $x_B = \frac{Q^2}{2p \cdot q}$
- x longitudinal momentum fraction carried by the active quark.
- $\xi \sim \frac{x_B}{2 - x_B}$ the longitudinal momentum transfer.
- $t = (p - p')^2$ squared momentum transfer to the nucleon.

The GPDs enter the DVCS amplitude through a complex integral. This integral is called a *Compton form factor* (CFF).

$$\mathcal{H}(\xi, t) = \int_{-1}^{1} H(x, \xi, t) \left(\frac{1}{\xi - x - i\epsilon} - \frac{1}{\xi + x - i\epsilon} \right) dx \ .$$

Photon electroproduction and GPDs

Experimentally we measure the cross section of the process $ep \to ep\gamma$.

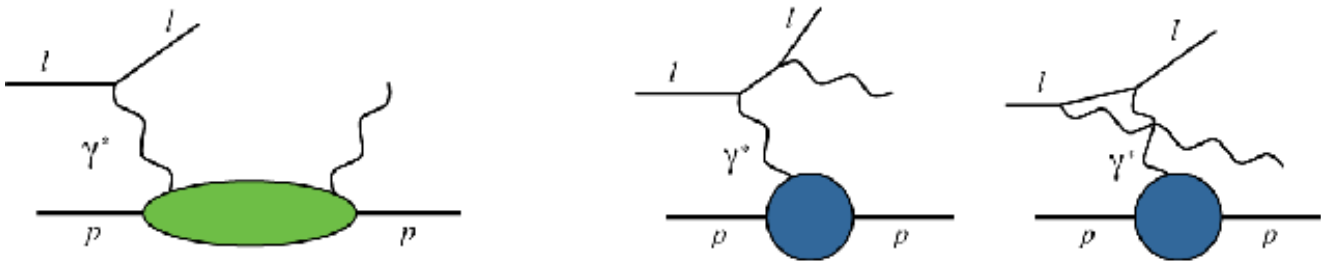

DVCS Bethe-Heitler

$$\frac{d^4\sigma(\lambda,\pm e)}{dQ^2 dx_B dt d\phi} = \frac{d^2\sigma_0}{dQ^2 dx_B}\frac{2\pi}{e^6} \times \left[\left|\mathcal{T}^{BH}\right|^2 + \left|\mathcal{T}^{DVCS}\right|^2 \mp \mathcal{I}\right] ,$$

with λ the helicity of the electron.

The Bethe-Heitler is known since it is QED process + Form factors from elastic scattering experiments.

A parameterization of cross section

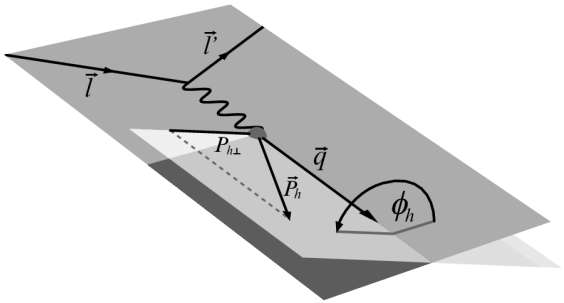

We can partially unfold the contributions, studying the ϕ-dependence.

$$|\mathcal{T}^{BH}|^2 = \frac{e^6 \sum_{n=0}^{2} c_n^{BH} \cos(n\phi)}{x_B^2 t y^2 (1+\epsilon^2)^2 \mathcal{P}_1(\phi)\mathcal{P}_2(\phi)} \quad \leftarrow \text{KNOWN!}$$

$$\left|\mathcal{T}^{DVCS}\right|^2 = \frac{e^6}{y^2 Q^2}\left\{c_0^{DVCS} + \sum_{n=1}^{2}\left[c_n^{DVCS}\cos(n\phi) + \lambda s_1^{DVCS}\sin(n\phi)\right]\right\}$$

$$\mathcal{I} = \frac{e^6}{x_B y^3 \mathcal{P}_1(\phi)\mathcal{P}_2(\phi) t}\left\{c_0^{\mathcal{I}} + \sum_{n=1}^{3}\left[c_n^{\mathcal{I}}\cos(n\phi) + \lambda s_n^{\mathcal{I}}\sin(n\phi)\right]\right\}$$

A parameterization of cross section

The CFFs are encapsulated in c_n and s_n, offering a parameterization of the cross section. In the leading twist approximation for unpolarized target:

$$c_0^{DVCS} \propto \mathcal{C}^{DVCS}(\mathcal{F},\mathcal{F}^*) = 4(1-x_B)\mathcal{H}\mathcal{H}^* + \cdots \quad (1)$$

$$c_1^{\mathcal{I}} \propto Re\ \mathcal{C}^{\mathcal{I}}(\mathcal{F}) = F_1\ Re\mathcal{H} + \xi(F_1+F_2)\ Re\widetilde{\mathcal{H}} - \frac{t}{4M^2}F_2\ Re\mathcal{E}\,,$$

$$s_1^{\mathcal{I}} \propto Im\ \mathcal{C}^{\mathcal{I}}(\mathcal{F}) = F_1\ Im\mathcal{H} + \xi(F_1+F_2)\ Im\widetilde{\mathcal{H}} - \frac{t}{4M^2}F_2\ Im\mathcal{E}\,,$$

By studying the ϕ-dependence of the observables, we can extract the CFFs. A lot of data have been collected in different kinematical regions (H1, ZEUS, Hermes, CLAS).

Mueller D., Belitsky A.V., Phys.Rev.D.82 (2010)

A fit global to disentangle all the CFFs

Kumericki and Muller performed a global fit of CFFs at leading-twist and leading-order (KM10a).

$$\Delta\sigma_{LU} \propto \sin\phi \times Im\left\{F_1\,\mathcal{H} + \xi(F_1+F_2)\,\widetilde{\mathcal{H}} - \frac{t}{4M^2}F_2\,\mathcal{E}\right\}, \tag{2}$$

$$\Delta\sigma_{UL} \propto \sin\phi \times Im\left\{F_1\,\widetilde{\mathcal{H}} + \xi(F_1+F_2)\left(\mathcal{H} + \frac{x_B}{2}\mathcal{E}\right) - \frac{t}{4M^2}F_2\,\widetilde{\mathcal{E}}\right\},$$

- the imaginary part of CFFs are given by beam or target spin asymmetries.
- the real parts are built using dispersion relations with the imaginary parts.

In january 2015, this fit was able to reproduce all the observables. Let's challenge it with high statistical precision DVCS data provided by Hall A (two experiments: 2004 and 2010).

The experimental setup

We want to study $ep \rightarrow ep\gamma$:

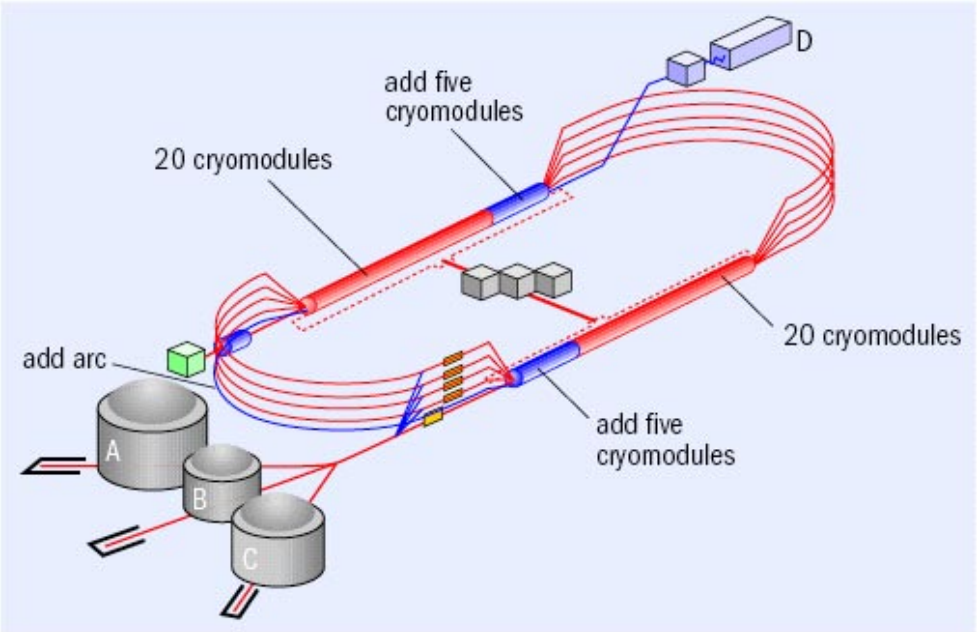

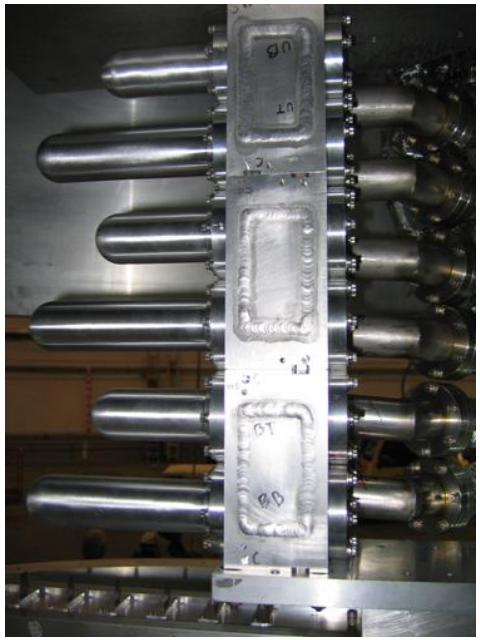

The accelerator provided:

- 80% longitudinally polarized electron beam on a 15 cm-long LH_2 target,
- with a maximal beam current of 200 μA (I<4 μA),
- up to 6 GeV (now 12 GeV).

The experimental setup

We want to study $ep \rightarrow ep\gamma$:

In the Hall A,

- The scattered electron is detected by a High Resolution Spectrometer (HRS): We measure accurately x_B and Q^2.
- The photon is detected by an electromagnetic calorimeter: The 4-momenta of the scattered electron and the photon gives t and ϕ.

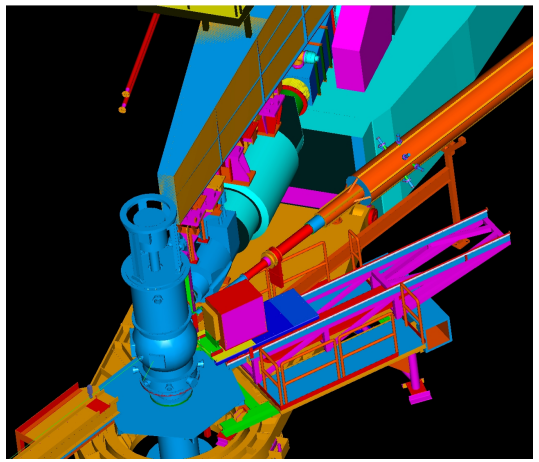

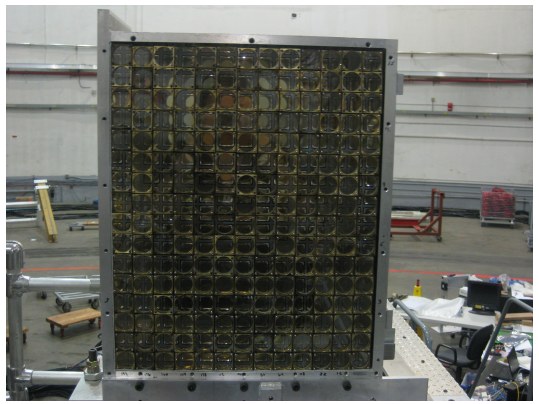

$N_{M_X^2 < M_{cut}^2} = N_{ep \to ep\gamma} + N_{acc} + N_{\pi^0 - 1\gamma} + N_{SIDIS}$

- N_{SIDIS} cannot be subtracted and we need to cut low enough in missing mass to have:

$$N_{SIDIS} << N_{ep \to e\gamma p}$$

- The fraction of exclusive events lost with the cut is corrected through the Monte-Carlo simulation.

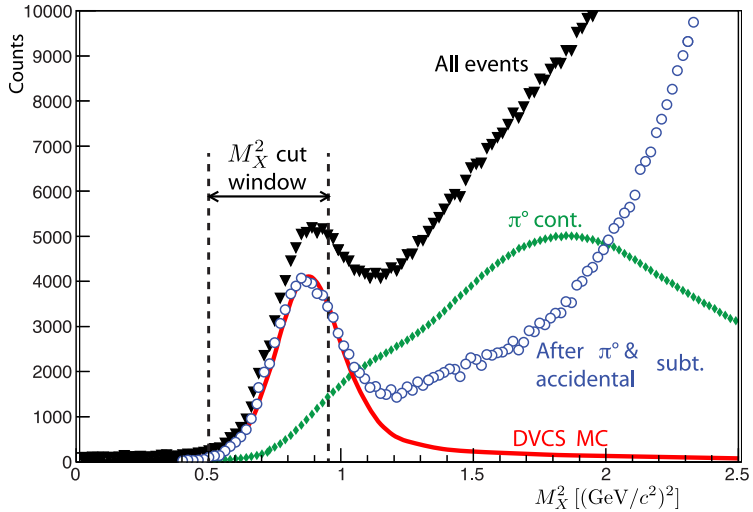

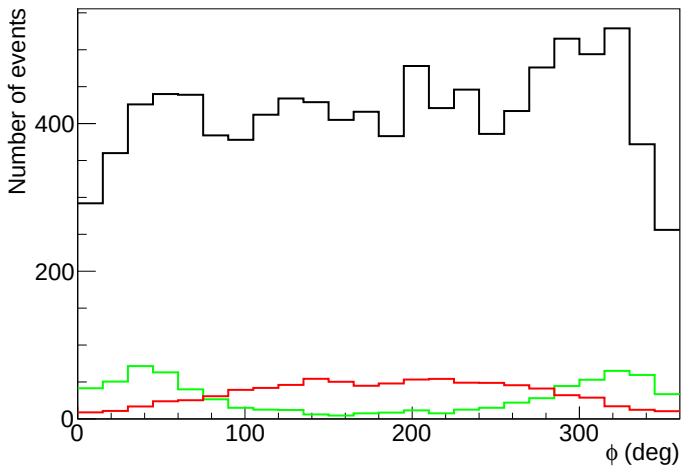

Here are the results from 2004!

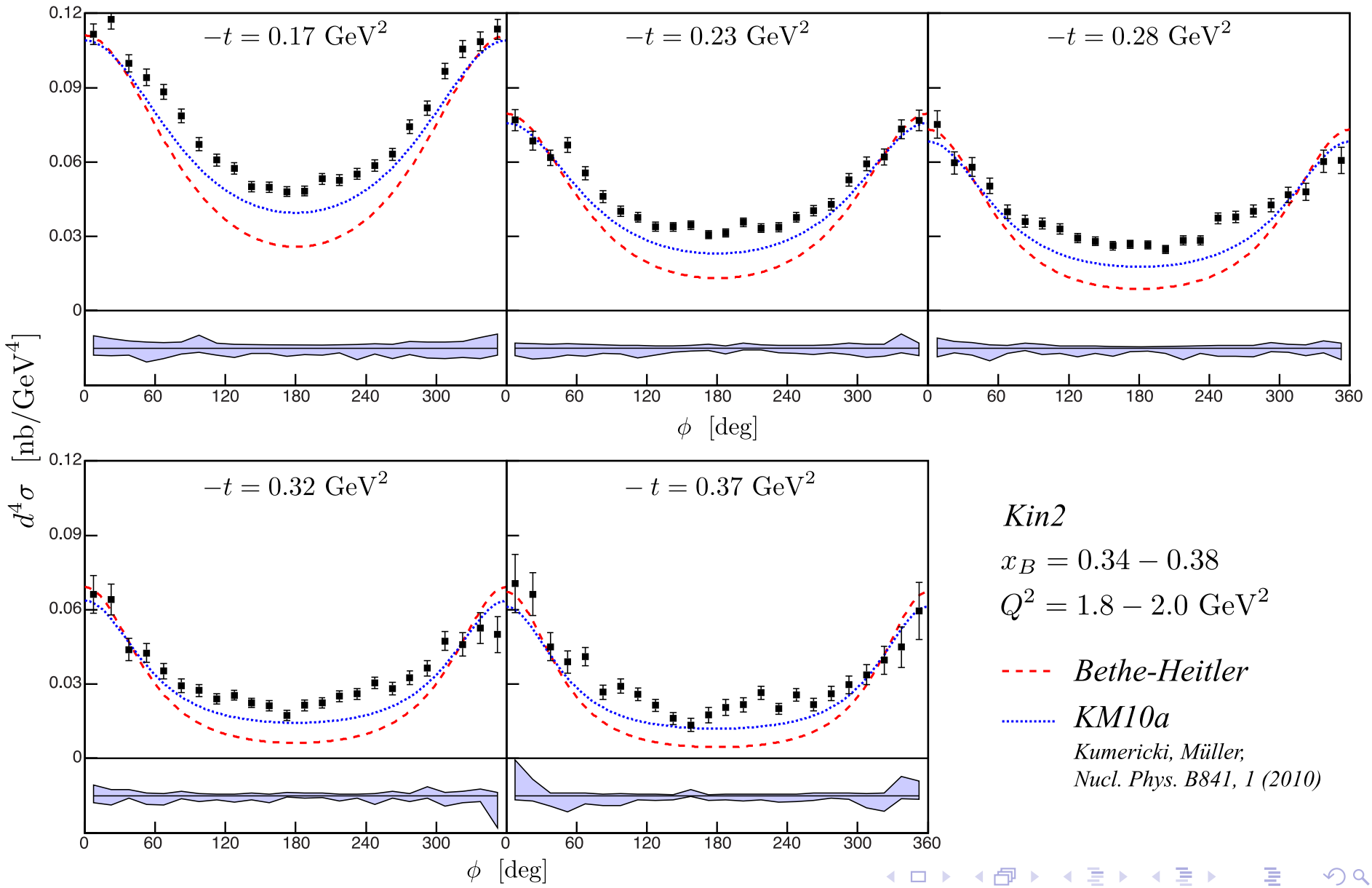

Kin2

$x_B = 0.34 - 0.38$

$Q^2 = 1.8 - 2.0$ GeV^2

Bethe-Heitler

KM10a

Kumericki, Müller, Nucl. Phys. B841, 1 (2010)

Here are the results from 2004!

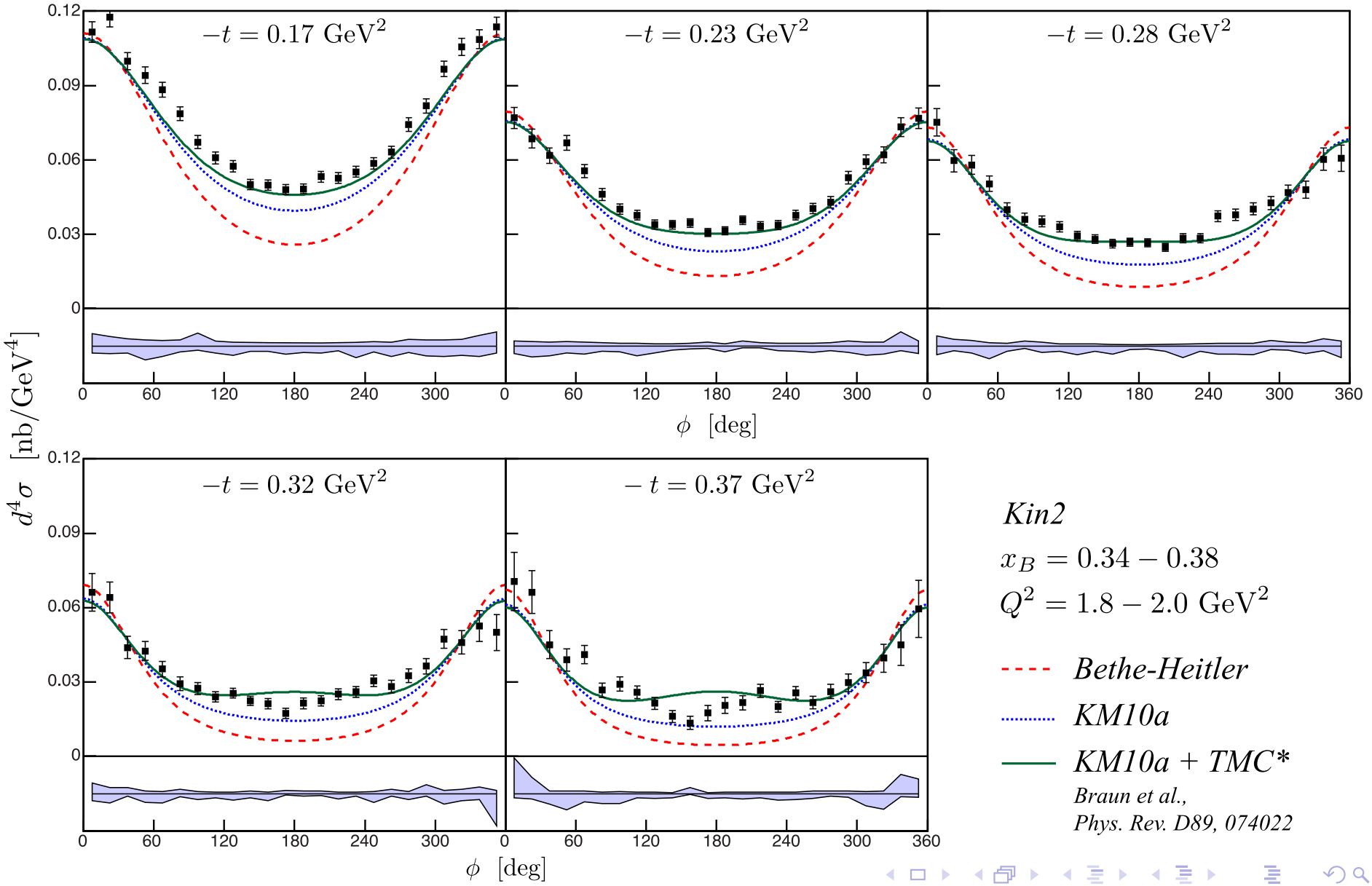

A lot of new DVCS data from 2004 Hall A experiment

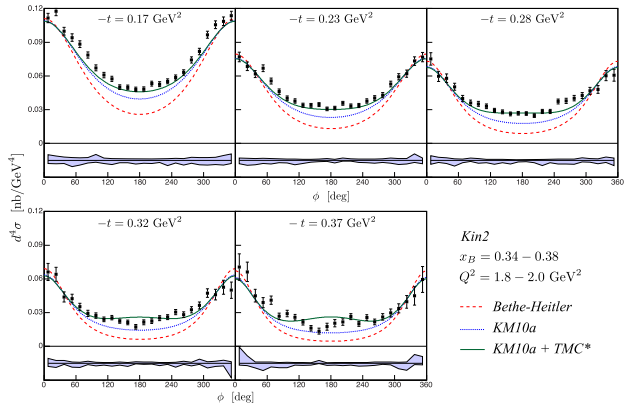

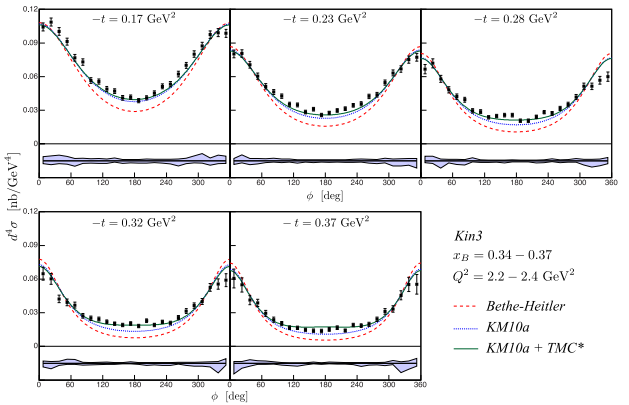

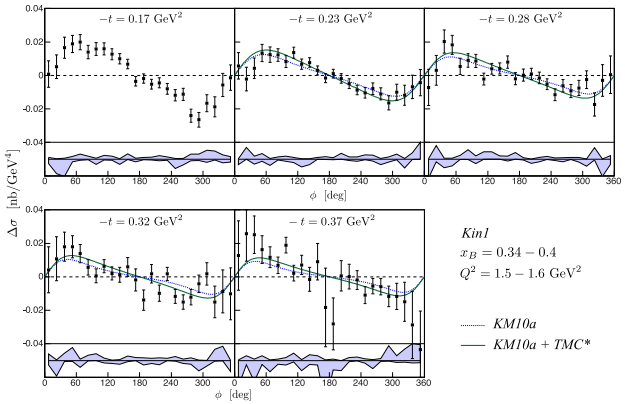

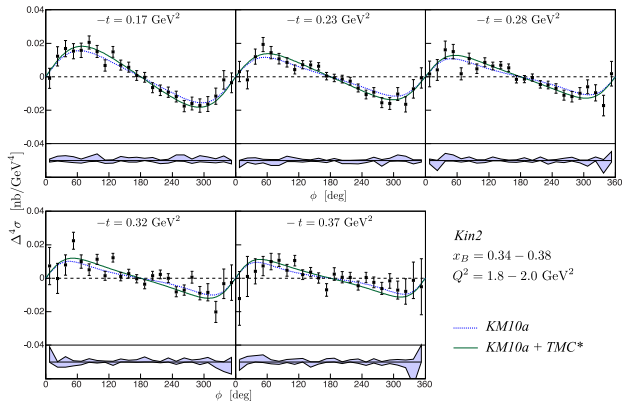

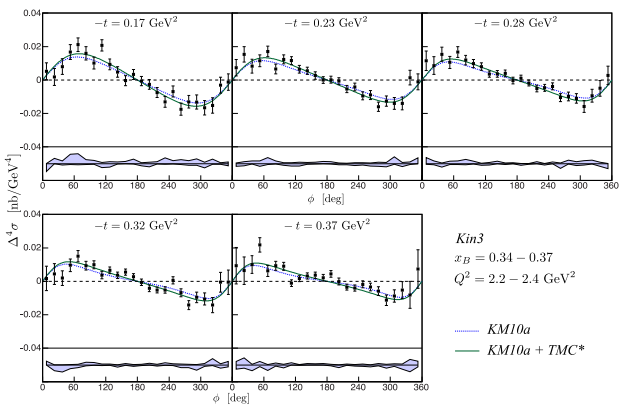

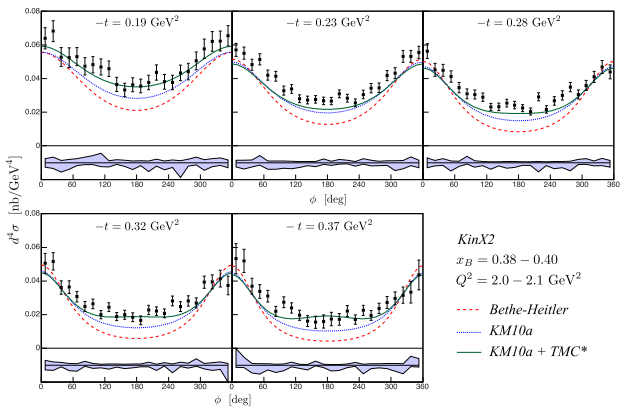

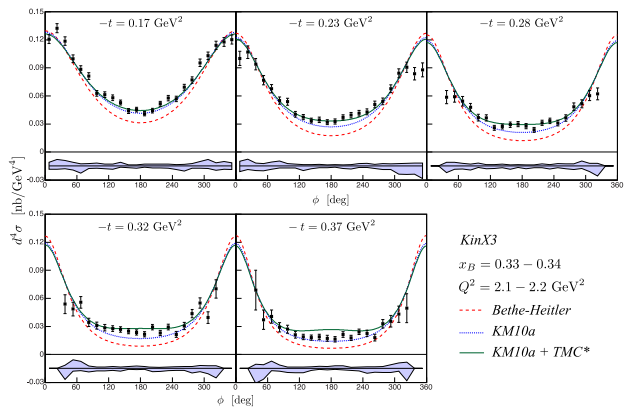

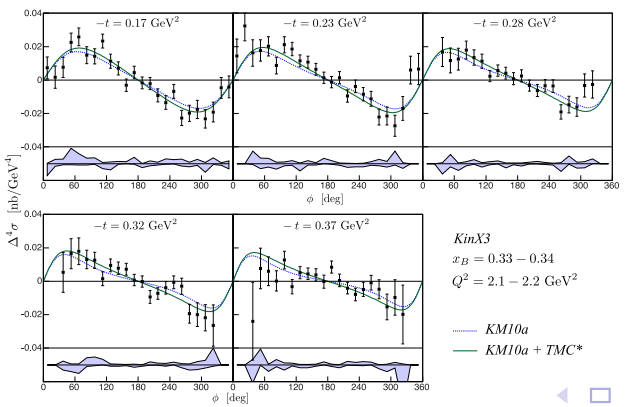

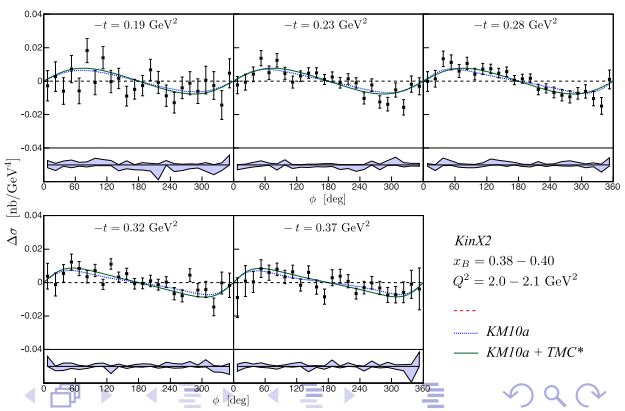

Where do the kinematical power corrections come from?

Belitsky, Muller and Ji decomposed the DVCS amplitude in helicity amplitude, using the lab frame as reference frame. In the BMJ formalism, the cross section is parametrized by a set of CFFs:

$$\mathcal{F}_{\mu\nu} \in \left\{ \mathcal{H}_{\mu\nu}, \mathcal{E}_{\mu\nu}, \tilde{\mathcal{H}}_{\mu\nu}, \tilde{\mathcal{E}}_{\mu\nu} \right\} \tag{3}$$

where μ (ν) is the helicity of the virtual (real) photon. Therefore we can distinguish three cases:

- $\mathcal{F}_{++}$ are the *helicity-conserved CFFs*. They are the regular leading-twist CFFs which describes diagram for which virtual and real photon have the same helicity.
- $\mathcal{F}_{0+}$ are the *longitudinal-to-transverse helicity flip CFFs*. They are *twist-3* CFFs related to the contribution of the longitudinal polarization of the virtual photon.
- $\mathcal{F}_{-+}$ are the *transverse-to-transverse helicity flip CFFs*. At leading-order, these CFFs are *twist-4*. But at NLO order, these CFFs involves the *twist-2* gluon transversity GPDs.

Where do the kinematical power corrections come from?

In the BMP formalism, the reference frame is taken such as both photons have purely longitudinal momentum. This choice makes easier the inclusion of kinematically suppressed terms (in t/Q^2 or M^2/Q^2). In the BMP formalism, the cross section is parametrized by a set of CFFs:

$$\mathbb{F}_{\mu\nu} \in \left\{ \mathbb{H}_{\mu\nu}, \mathbb{E}_{\mu\nu}, \tilde{\mathbb{H}}_{\mu\nu}, \tilde{\mathbb{E}}_{\mu\nu} \right\} \tag{4}$$

where μ (ν) is the helicity of the virtual (real) photon. Therefore we can distinguish three cases:

- $\mathbb{F}_{++}$ are the *helicity-conserved CFFs*. They are twist-2 CFFs.
- $\mathbb{F}_{0+}$ are the *longitudinal-to-transverse helicity flip CFFs*. They are *twist-3* CFFs.
- $\mathbb{F}_{-+}$ are the *transverse-to-transverse helicity flip CFFs*. At LO, these CFFs are *twist-4*. At NLO, these CFFs involves the gluon transversity GPDs.

BMP... BMJ... which difference?

But let's stay at leading-order. The BMP CFFs are not the same as the BMJ CFFs. The BMP CFFs are more complex terms. As an example, $\mathbb{H}_{++}$, we have:

$$\mathcal{H}_{++} = T_0 \otimes H \,, \tag{5}$$

$$\mathbb{H}_{++} = T_0 \otimes H + \frac{-t}{Q^2}\left[\frac{1}{2}T_0 - T_1 - 2\xi D_\xi T_2\right] \otimes H + \frac{2t}{Q^2}\xi^2 \partial_\xi T_2 \otimes (H+E) \,. \tag{6}$$

We can go from BMP to BMJ CFFs by making the following replacement:

$$\mathcal{F}_{++} = \mathbb{F}_{++} + \frac{\chi}{2}\left[\mathbb{F}_{++} + \mathbb{F}_{-+}\right] - \chi_0 \mathbb{F}_{0+} \,, \tag{7}$$

$$\mathcal{F}_{-+} = \mathbb{F}_{-+} + \frac{\chi}{2}\left[\mathbb{F}_{++} + \mathbb{F}_{-+}\right] - \chi_0 \mathbb{F}_{0+} \,, \tag{8}$$

$$\mathcal{F}_{0+} = -(1+\chi)\mathbb{F}_{0+} + \chi_0\left[\mathbb{F}_{++} + \mathbb{F}_{-+}\right] \,, \tag{9}$$

with: $\chi_0 \propto \sqrt{t'}/Q$ and $\chi \propto t'/Q^2$. The leading-twist assumption gives different results between BMP and BMJ.

Differences in the LT-LO assumption: BMJ

Assuming leading-twist and LO in BMJ, we have $\mathcal{F}_{-+} = 0$ and $\mathcal{F}_{0+} = 0$. It is important when regarding the DVCS amplitude. We have:

$$c_{0,\mathrm{unp}}^{\mathrm{VCS}} = 2\frac{2-2y+y^2+\frac{\epsilon^2}{2}y^2}{1+\epsilon^2}\,\mathcal{C}_{\mathrm{unp}}^{\mathrm{VCS}}(\mathcal{F}_{\pm+},\mathcal{F}_{\pm+}^*) + 8\frac{1-y-\frac{\epsilon^2}{4}y^2}{1+\epsilon^2}\,\mathcal{C}_{\mathrm{unp}}^{\mathrm{VCS}}(\mathcal{F}_{0+},\mathcal{F}_{0+}^*)\,, \tag{10}$$

$$\begin{Bmatrix} c_{1,\mathrm{unp}}^{\mathrm{VCS}} \\ s_{1,\mathrm{unp}}^{\mathrm{VCS}} \end{Bmatrix} = \frac{4\sqrt{2}\sqrt{1-y-\frac{\epsilon^2}{4}y^2}}{1+\epsilon^2} \begin{Bmatrix} 2-y \\ -\lambda y\sqrt{1+\epsilon^2} \end{Bmatrix} \begin{Bmatrix} \Re\mathrm{e} \\ \Im\mathrm{m} \end{Bmatrix} \mathcal{C}_{\mathrm{unp}}^{\mathrm{VCS}}\left(\mathcal{F}_{0+}\middle|\mathcal{F}_{++}^*,\mathcal{F}_{-+}^*\right), \tag{11}$$

$$c_{2,\mathrm{unp}}^{\mathrm{VCS}} = 8\frac{1-y-\frac{\epsilon^2}{4}y^2}{1+\epsilon^2}\,\Re\mathrm{e}\,\mathcal{C}_{\mathrm{unp}}^{\mathrm{VCS}}\left(\mathcal{F}_{-+},\mathcal{F}_{++}^*\right). \tag{12}$$

which reduces to:

$$c_{0,\mathrm{unp}}^{\mathrm{VCS}} = 2\frac{2-2y+y^2+\frac{\epsilon^2}{2}y^2}{1+\epsilon^2}\,\mathcal{C}_{\mathrm{unp}}^{\mathrm{VCS}}(\mathcal{F}_{++},\mathcal{F}_{++}^*) \tag{13}$$

The DVCS amplitude is ϕ-**independent** with a **single** beam-energy dependence.

Differences in the LT-LO assumption: BMP

Assuming leading-twist and LO in BMP, we have $\mathbb{F}_{-+} = 0$ and $\mathbb{F}_{0+} = 0$.

$$\mathcal{F}_{++} = \left(1 + \tfrac{\chi}{2}\right) \mathbb{F}_{++} \,, \tag{14}$$

$$\mathcal{F}_{-+} = \tfrac{\chi}{2} \mathbb{F}_{++} \,, \tag{15}$$

$$\mathcal{F}_{0+} = \chi_0 \mathbb{F}_{++} \,, \tag{16}$$

It is important when looking at the DVCS amplitude.

$$c^{\mathrm{VCS}}_{0,\mathrm{unp}} = 2 \frac{2 - 2y + y^2 + \frac{\epsilon^2}{2} y^2}{1 + \epsilon^2} \mathcal{C}^{\mathrm{VCS}}_{\mathrm{unp}}(\mathcal{F}_{\pm+}, \mathcal{F}^*_{\pm+}) + 8 \frac{1 - y - \frac{\epsilon^2}{4} y^2}{1 + \epsilon^2} \mathcal{C}^{\mathrm{VCS}}_{\mathrm{unp}}(\mathcal{F}_{0+}, \mathcal{F}^*_{0+}) \,, \tag{17}$$

$$\begin{Bmatrix} c^{\mathrm{VCS}}_{1,\mathrm{unp}} \\ s^{\mathrm{VCS}}_{1,\mathrm{unp}} \end{Bmatrix} = \frac{4\sqrt{2}\sqrt{1 - y - \frac{\epsilon^2}{4} y^2}}{1 + \epsilon^2} \begin{Bmatrix} 2 - y \\ -\lambda y \sqrt{1 + \epsilon^2} \end{Bmatrix} \begin{Bmatrix} \Re\mathrm{e} \\ \Im\mathrm{m} \end{Bmatrix} \mathcal{C}^{\mathrm{VCS}}_{\mathrm{unp}} \left(\mathcal{F}_{0+} \middle| \mathcal{F}^*_{++}, \mathcal{F}^*_{-+}\right) , \tag{18}$$

$$c^{\mathrm{VCS}}_{2,\mathrm{unp}} = 8 \frac{1 - y - \frac{\epsilon^2}{4} y^2}{1 + \epsilon^2} \Re\mathrm{e}\, \mathcal{C}^{\mathrm{VCS}}_{\mathrm{unp}} \left(\mathcal{F}_{-+}, \mathcal{F}^*_{++}\right) . \tag{19}$$

The DVCS amplitude is **no longer** ϕ-independent with **multiple** beam-energy dependences.

Troubles for Rosenbluth separations in Hall A in 2010

If one wants to separate interference from DVCS^2 contributions by changing the beam energy, he will also change **the polarization of the virtual photon.** And considering the size of the corrections, we cannot neglect them to do a clean work... especially for Jefferson Lab kinematics!

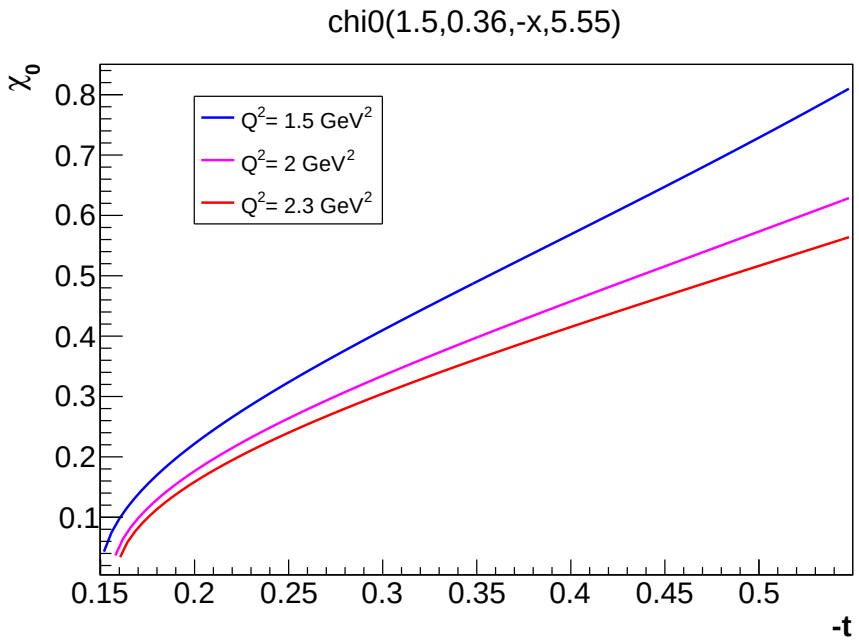

Since the kinematical power corrections are "helicity-dependent", it is crucial to take them into account to do the separation.

A Rosenbluth separation in Hall A in 2010?

In 2010, a new DVCS experiment in Hall A which aimed at separating the interference from the $DVCS^2$ contributions:

Setting	E (GeV)	Q^2 (GeV^2)	x_B	W (GeV)
2010-Kin1	(3.355 ; 5.55)	1.5	0.36	1.9
2010-Kin2	(4.455 ; 5.55)	1.75	0.36	2
2010-Kin3	(4.455 ; 5.55)	2	0.36	2.1

Since the data analysis is almost identical to the one for 2004, I am skipping it. Let's do the simplest test for LT/LO approach: we fit the real and imaginary parts of $\mathbb{H}_{++}\mathbb{E}_{++}\tilde{\mathbb{H}}_{++}\tilde{\mathbb{E}}_{++}$:

- simultaneously on unpolarized and polarized cross sections,
- simultaneously on the two beam energies,
- simultaneously for the three Q^2-values (but I neglect the Q-evolution),
- on one t-bin.

LT/LO approach: $\mathbb{H}_{++}$, $\mathbb{E}_{++}$, $\tilde{\mathbb{H}}_{++}$, $\tilde{\mathbb{E}}_{++}$

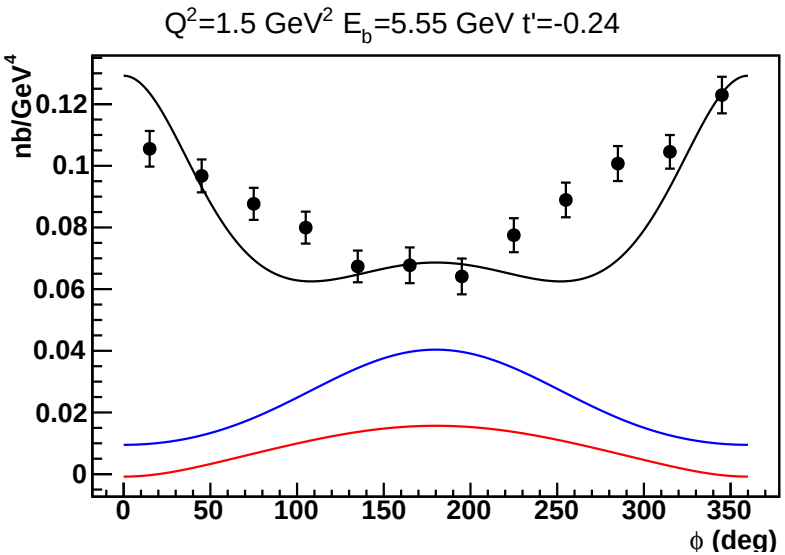

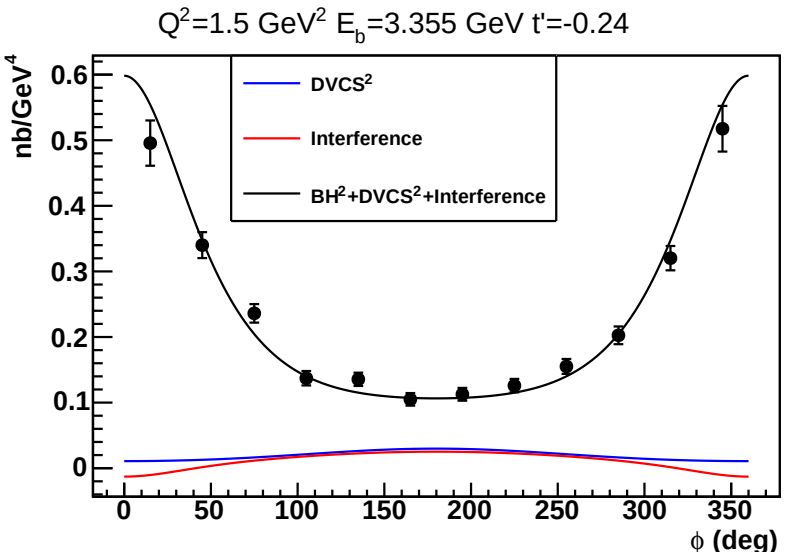

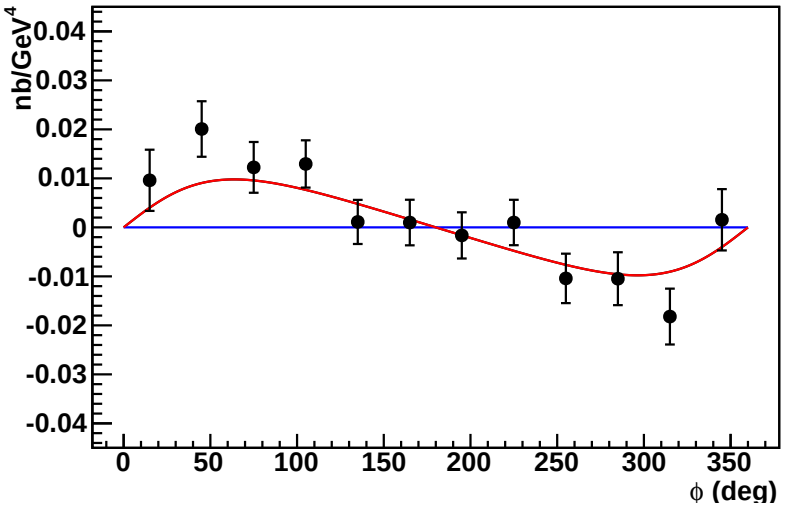

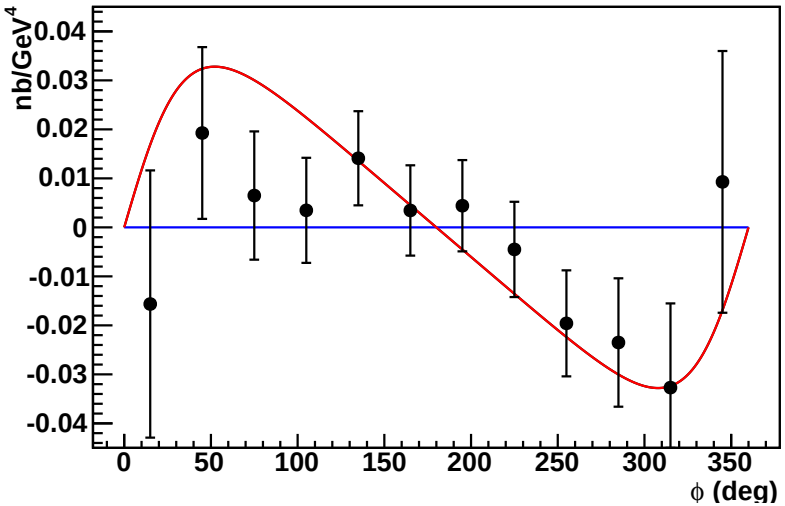

LT/LO approach: $\mathbb{H}_{++}$, $\mathbb{E}_{++}$, $\tilde{\mathbb{H}}_{++}$, $\tilde{\mathbb{E}}_{++}$

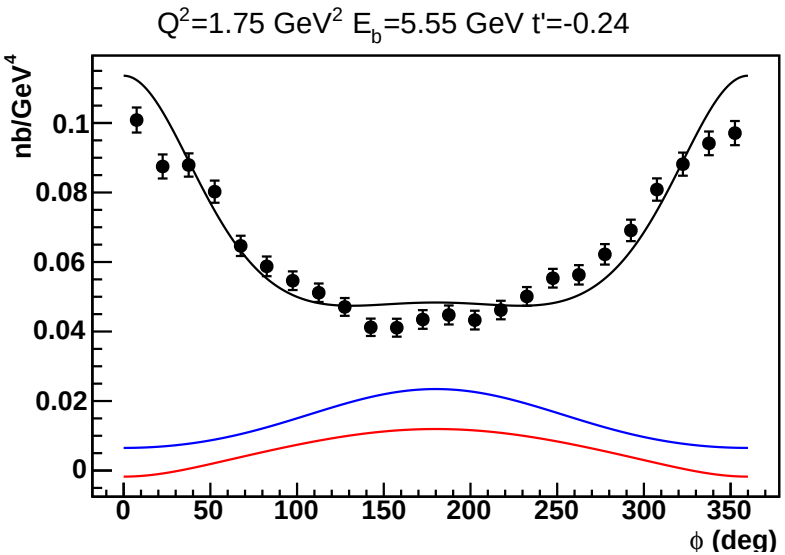

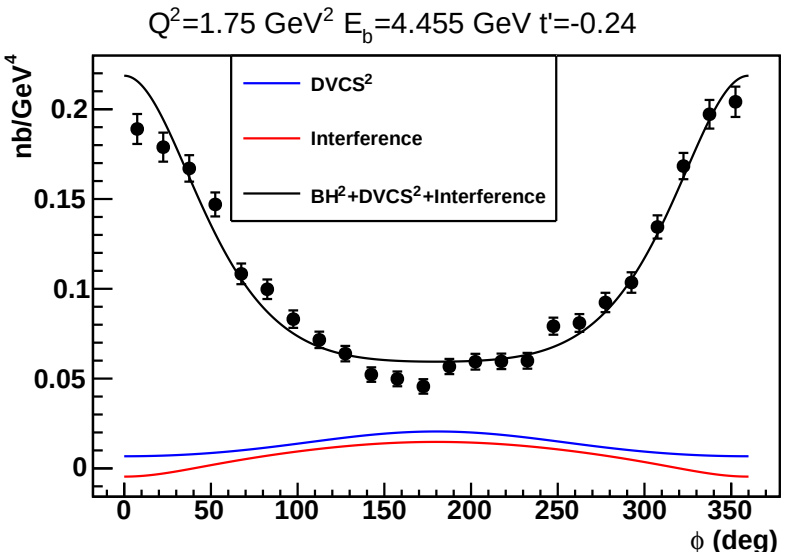

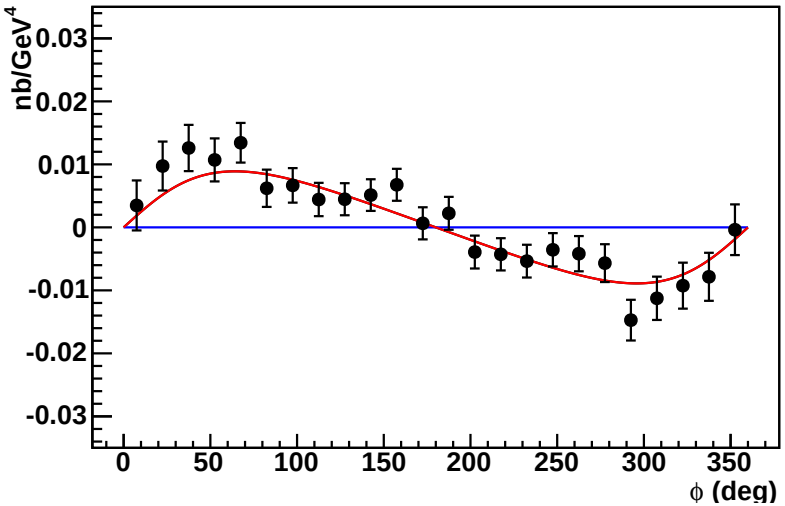

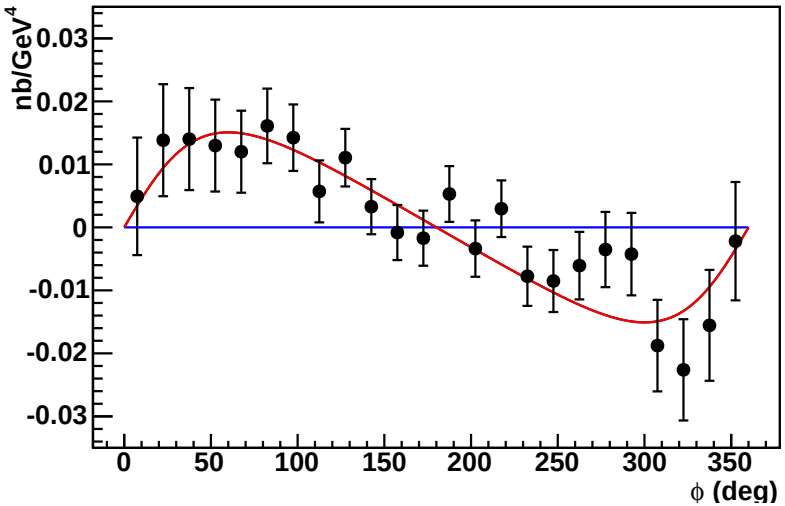

LT/LO approach: $\mathbb{H}_{++}$, $\mathbb{E}_{++}$, $\tilde{\mathbb{H}}_{++}$, $\tilde{\mathbb{E}}_{++}$

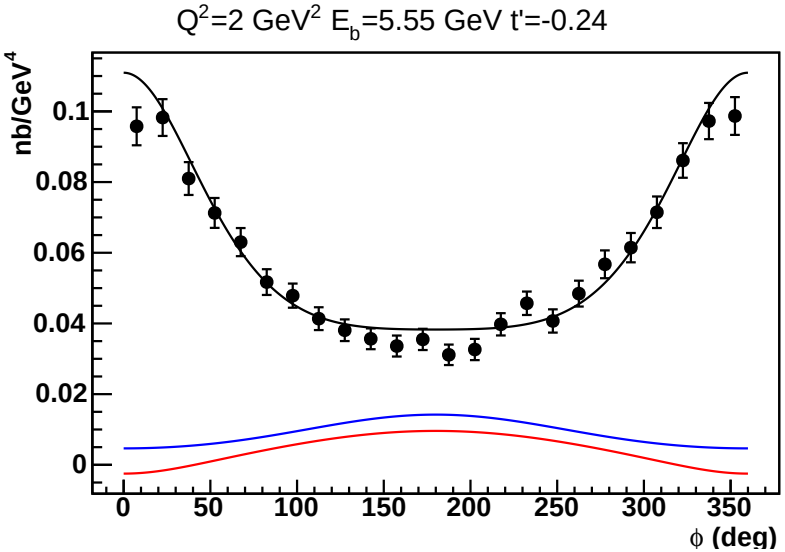

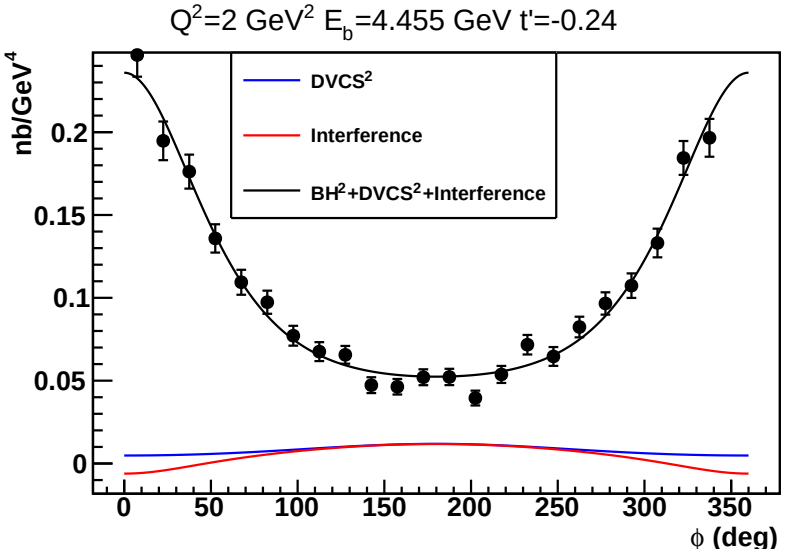

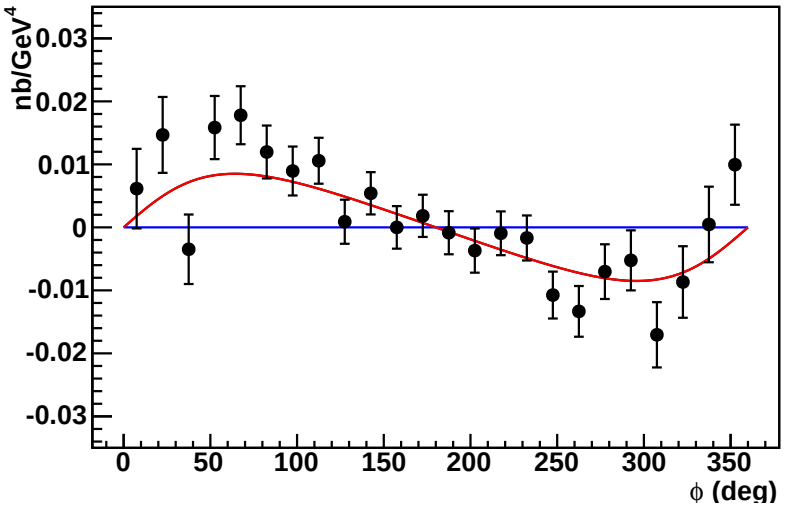

Some twist-3??: $\mathbb{H}_{++}$, $\tilde{\mathbb{H}}_{++}$, $\mathbb{H}_{0+}$, $\tilde{\mathbb{H}}_{0+}$

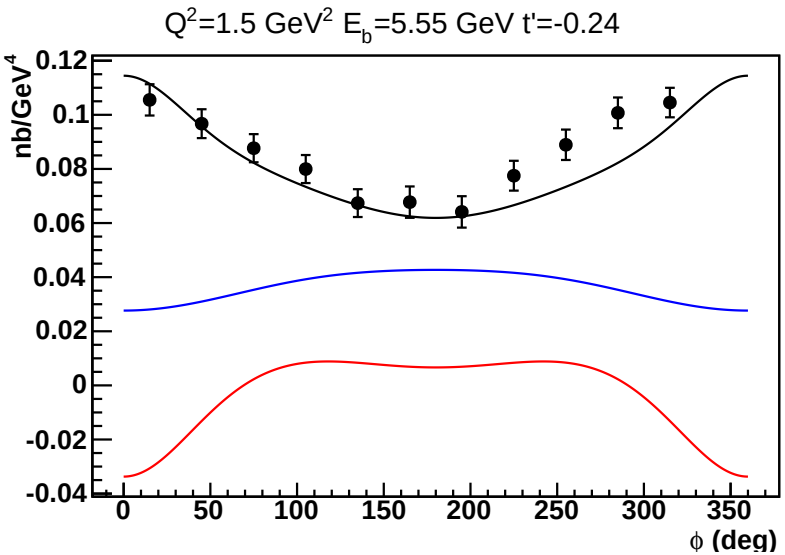

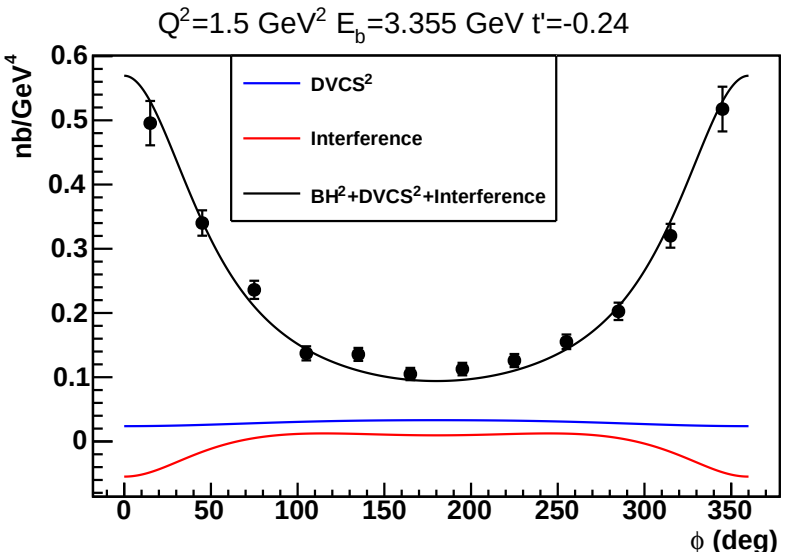

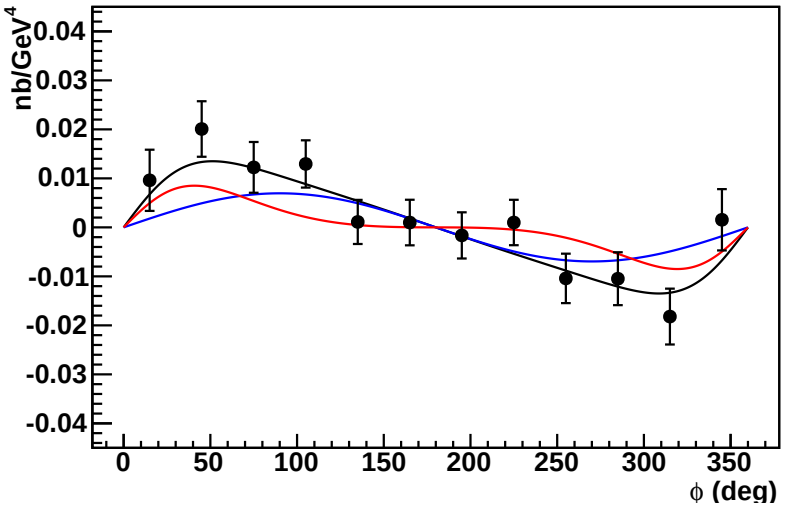

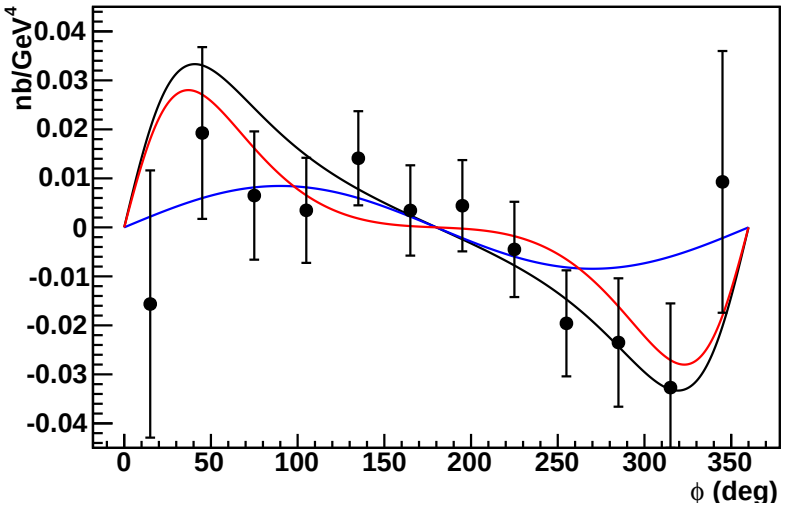

Some twist-3??: $\mathbb{H}_{++}$, $\tilde{\mathbb{H}}_{++}$, $\mathbb{H}_{0+}$, $\tilde{\mathbb{H}}_{0+}$

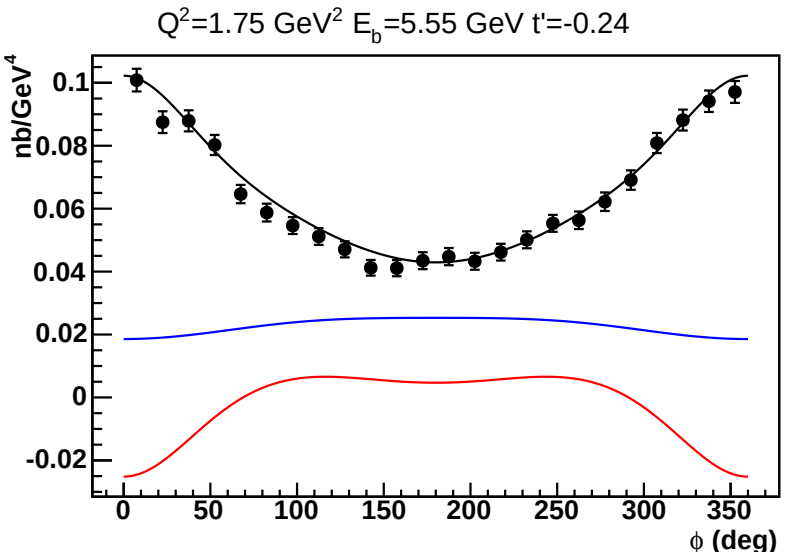

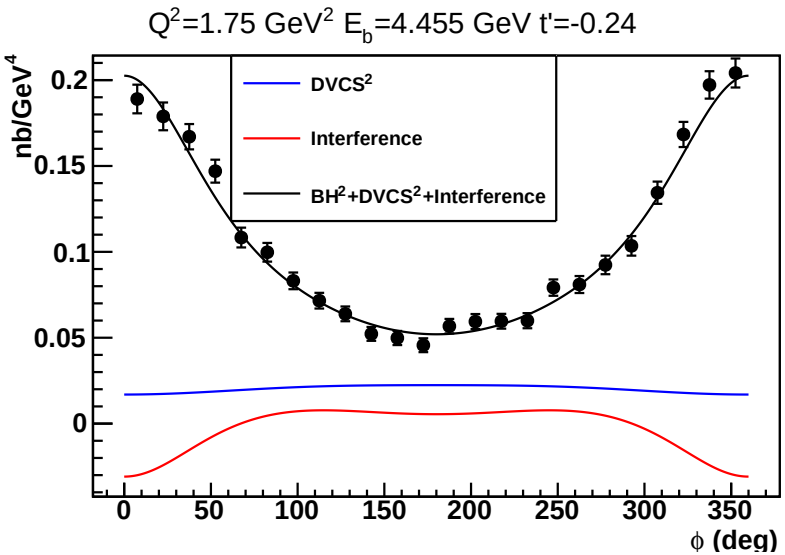

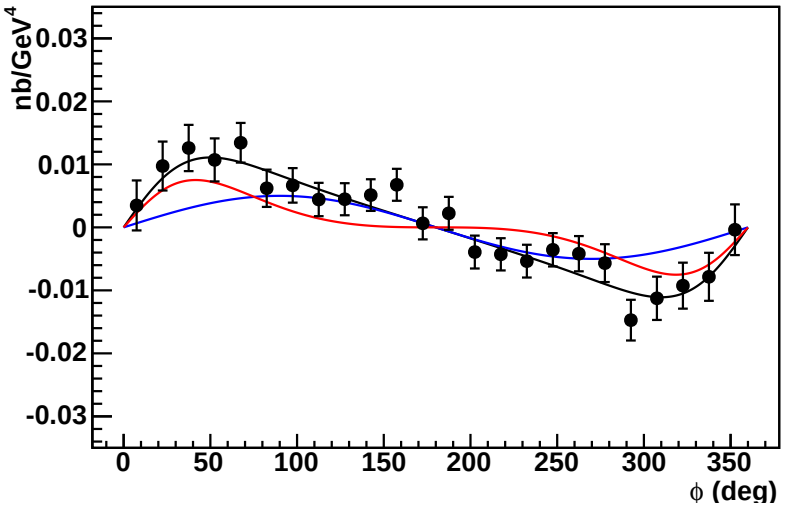

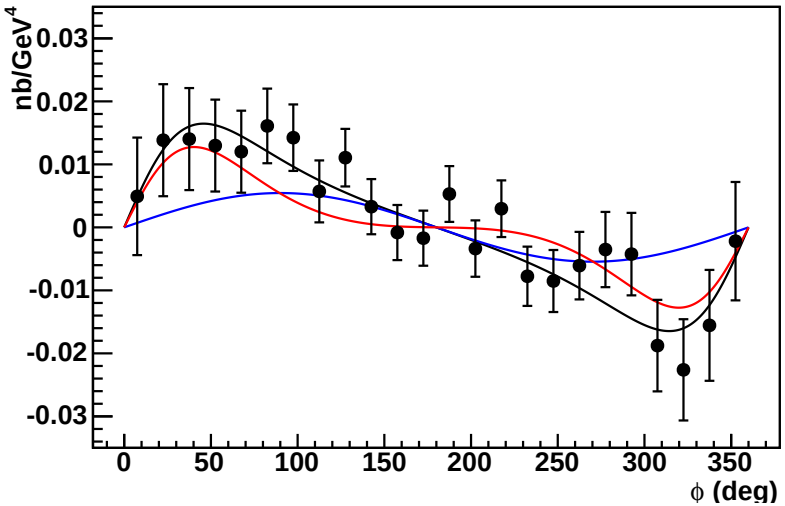

Some twist-3??: $\mathbb{H}_{++}$, $\tilde{\mathbb{H}}_{++}$, $\mathbb{H}_{0+}$, $\tilde{\mathbb{H}}_{0+}$

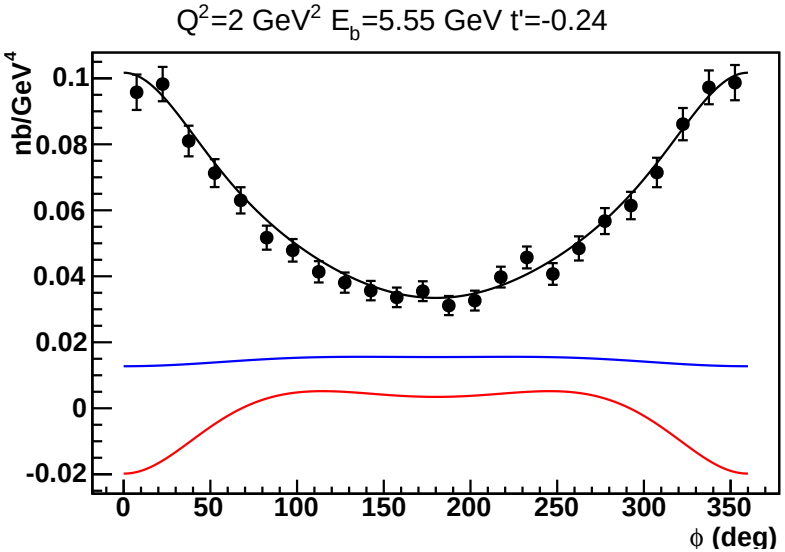

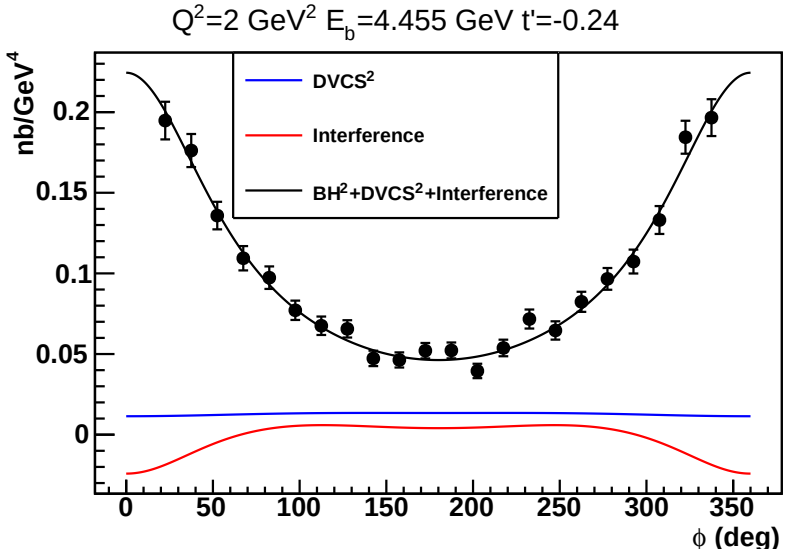

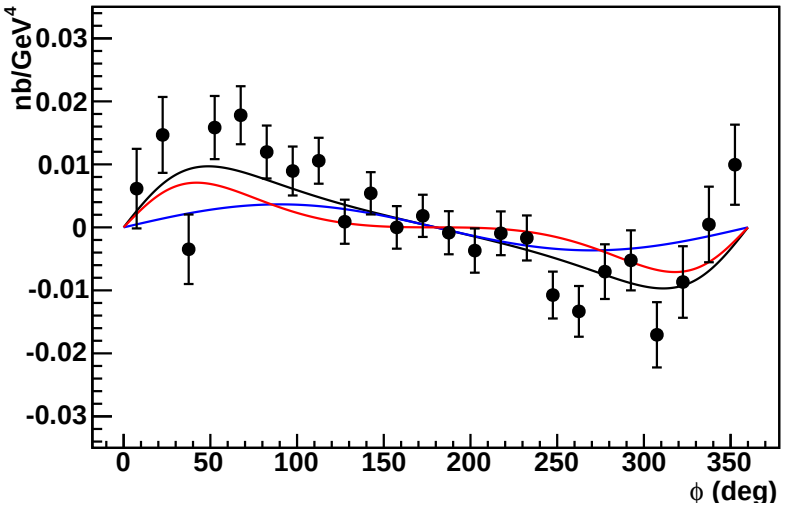

What about gluons at NLO: $\mathbb{H}_{++}$, $\tilde{\mathbb{H}}_{++}$, $\mathbb{H}_{-+}$, $\tilde{\mathbb{H}}_{-+}$

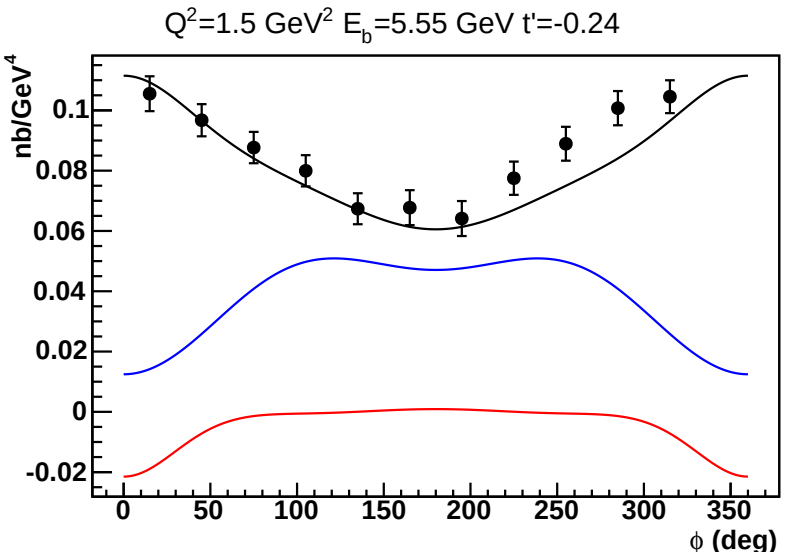

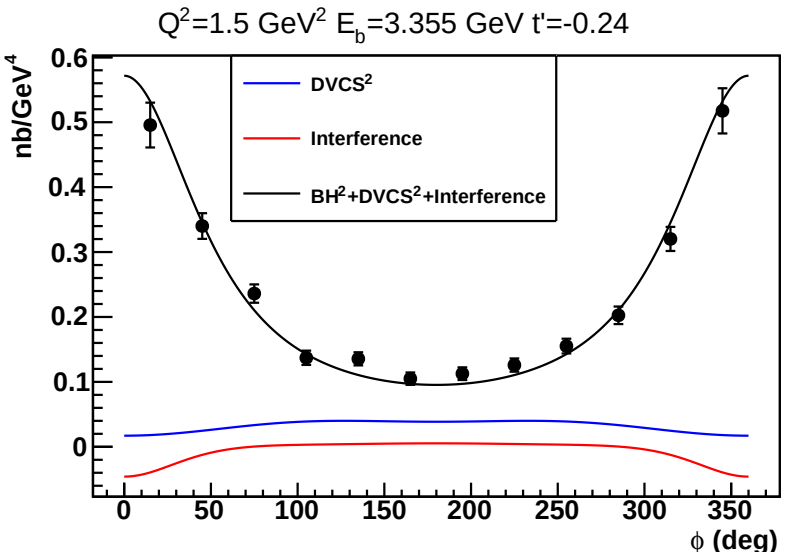

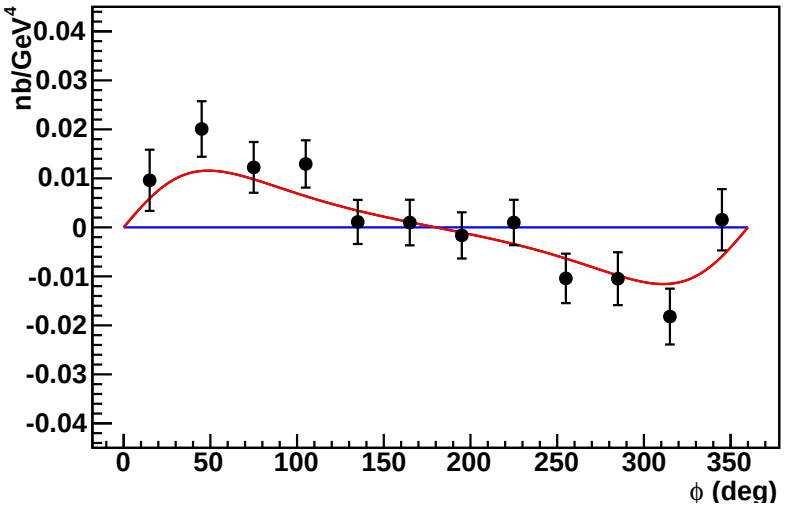

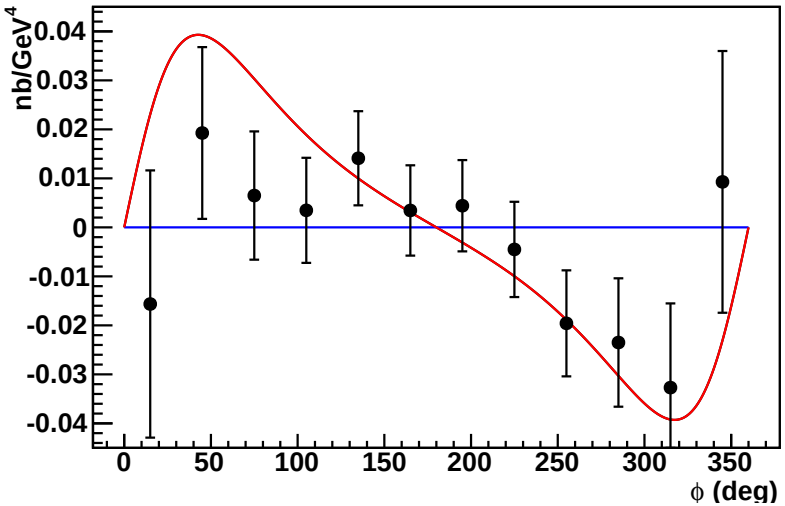

What about gluons at NLO: $\mathbb{H}_{++}$, $\tilde{\mathbb{H}}_{++}$, $\mathbb{H}_{-+}$, $\tilde{\mathbb{H}}_{-+}$

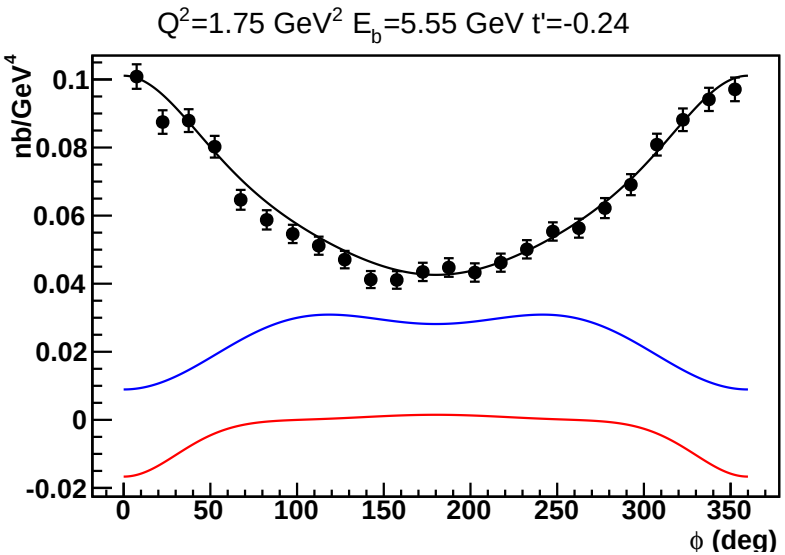

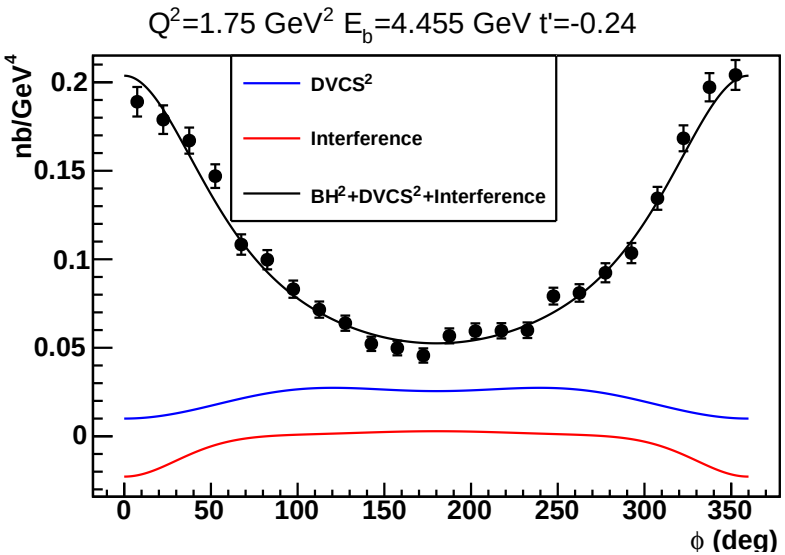

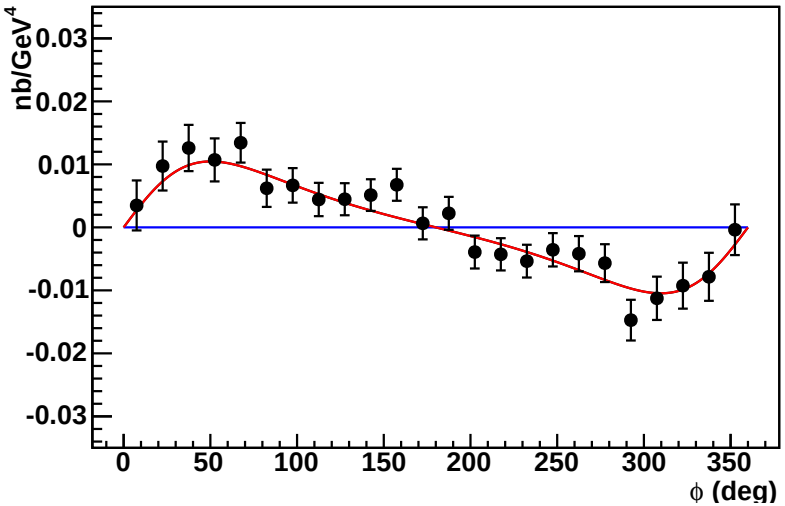

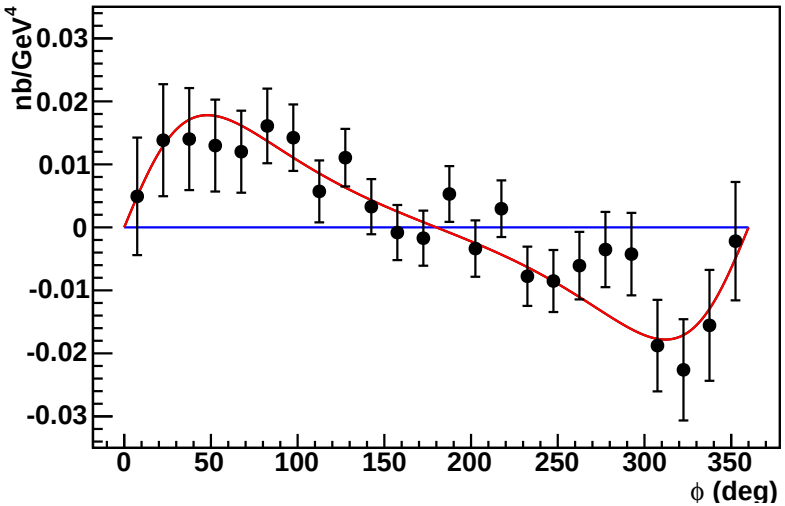

What about gluons at NLO: $\mathbb{H}_{++}$, $\tilde{\mathbb{H}}_{++}$, $\mathbb{H}_{-+}$, $\tilde{\mathbb{H}}_{-+}$

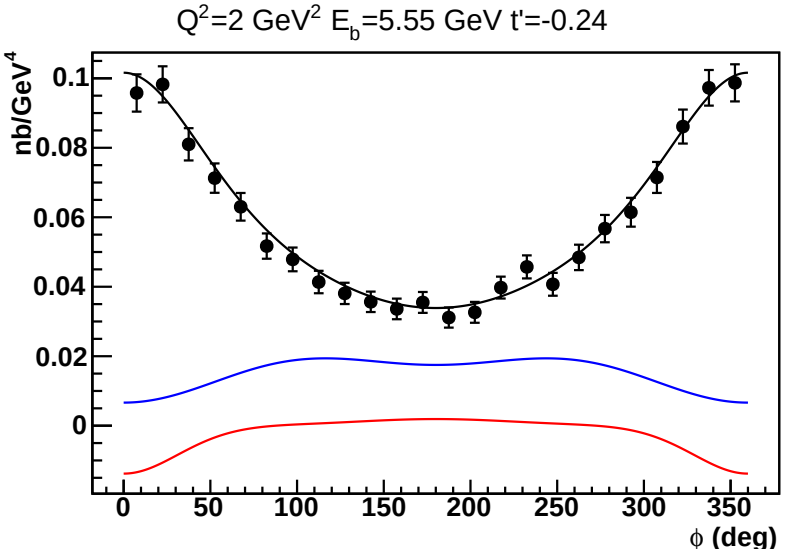

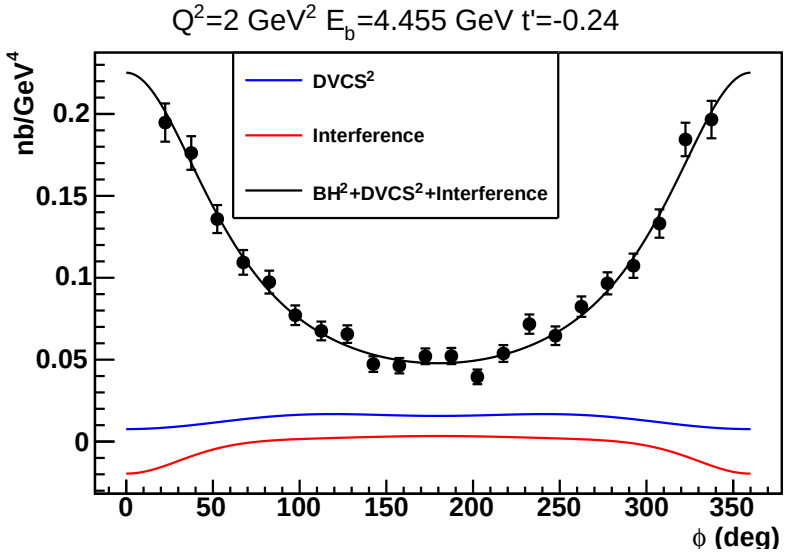

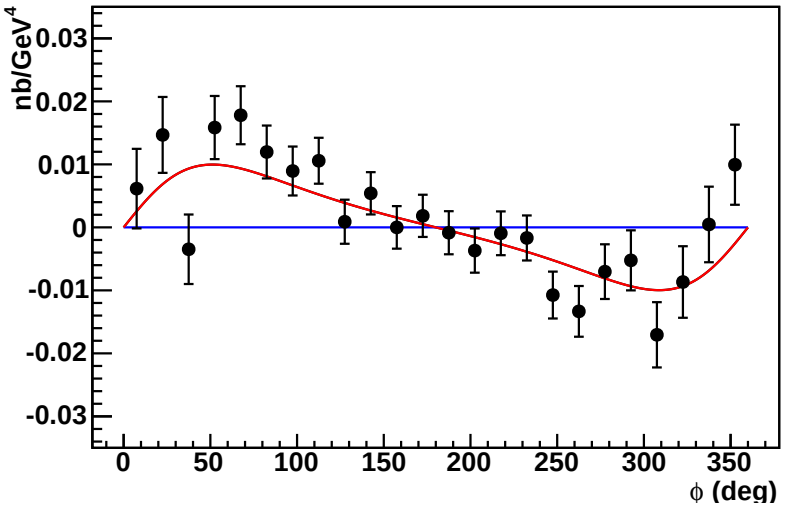

Conclusion

Kinematical power corrections must be taken into account to do a clean extraction of GPDs and tomography of the nucleon.

	LT-LO	0+	-+
χ^2/Ndf	461/208	245/208	244/208

It seems that there is higher-twist and/or Next-to-Leading order contributions in the JLab-6GeV data. Rosenbluth separation: Investigate the helicity structure of the DVCS!

What next? A fantastic DVCS program at 12 GeV (see Daria's talk)

- DVCS experiment in Hall A will soon be finished.
- Rosenbluth separation in CLAS12 (6.6, 8.8 and 11 GeV).
- Rosenbluth separation in Hall C.
- EIC? Let's see what happens in the next 5 years.

All together, the three halls will give us a precise idea of the GPDs in the valence region.

Thank you!

The experimental setup

We want to study $ep \to ep\gamma$:

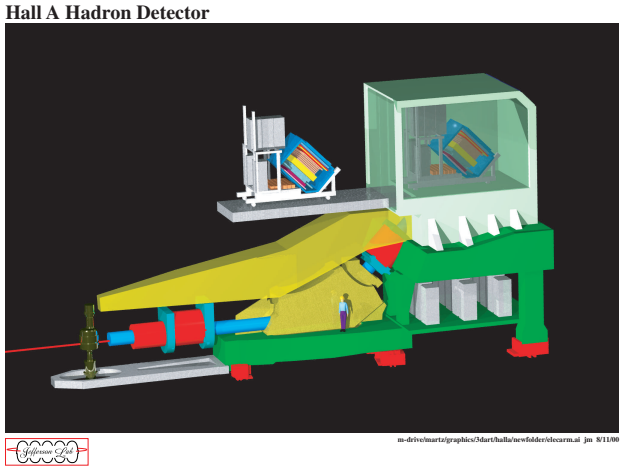

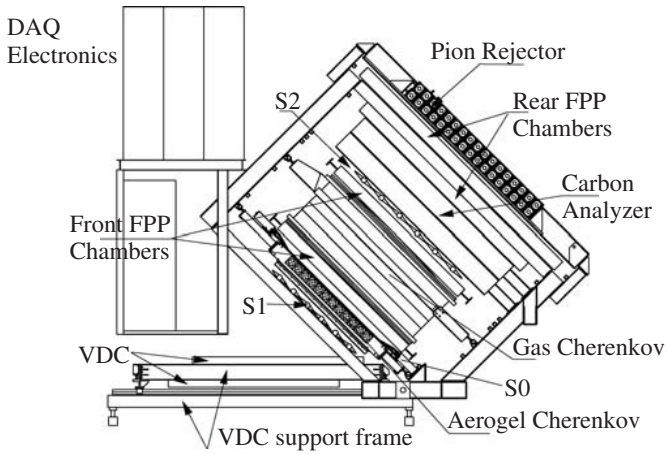

The High Resolution spectrometer detects and characterizes the scattered electron:
$\frac{\delta p}{p} \simeq 2.10^{-4}$ and solid angle $\simeq 6$ msr.

It allows an accurate measurement of Q^2 and x_B.

Scintillators and Čerenkov detector were part of the trigger.

$N_{M_X^2 < M_{cut}^2} = N_{ep \to ep\gamma} + N_{acc} + N_{\pi^0 - 1\gamma} + N_{SIDIS}$

[noframenumbering]

Accidentals are time-independent.

Estimated by studying events outside of the coincidence window.

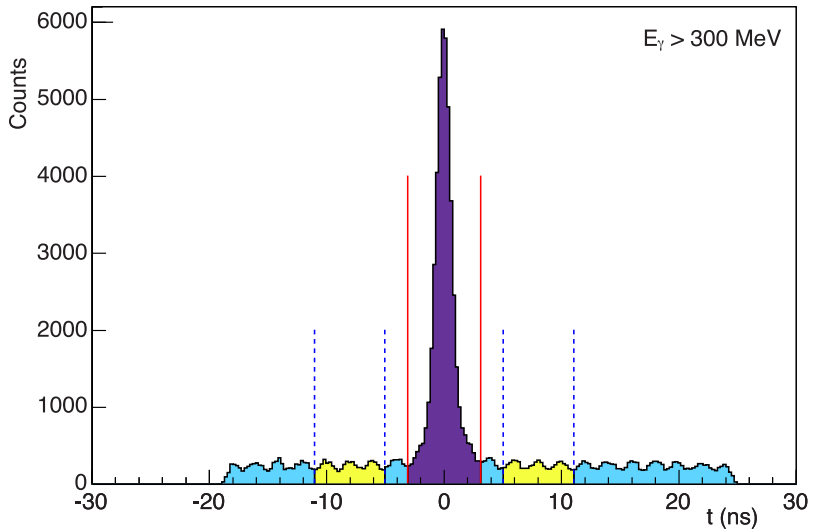

Accidentals are mostly located around $\phi = 0°$. We require a missing mass higher than 0.5 GeV^2 to reduce the statistical uncertainty from the subtraction.

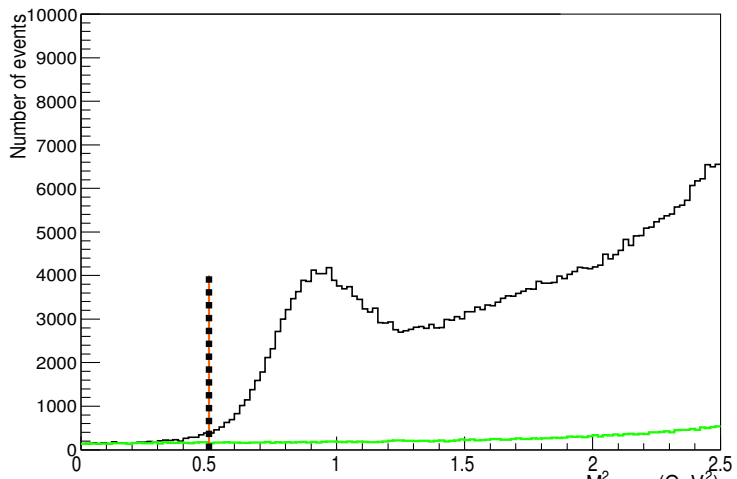

$N_{M_X^2<M_{cut}^2} = N_{ep\to ep\gamma} + N_{acc} + N_{\pi^0-1\gamma} + N_{SIDIS}$

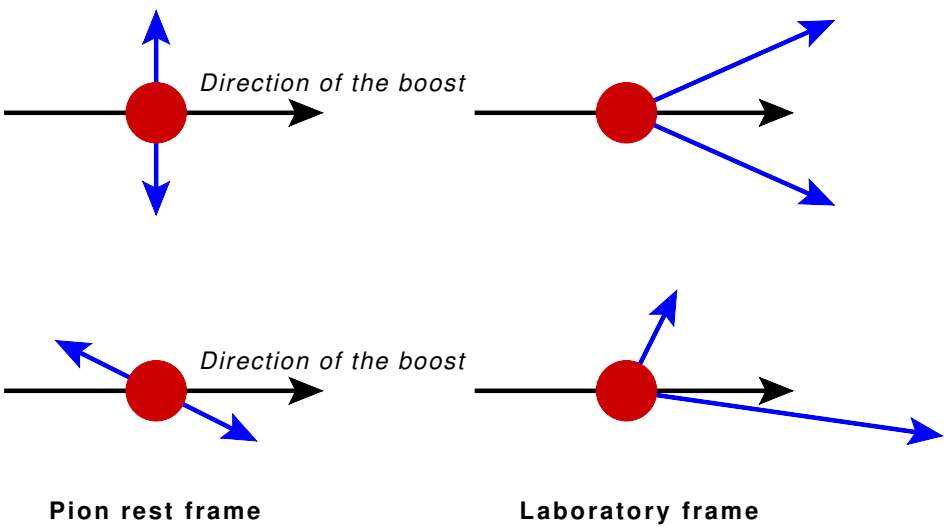

The kinetic energy of the π^0 is shared between the two photons depending on their direction with respect to the π^0 momentum.

We just need to evaluate the phase space of decay contributing to the contamination.

Principle: For each detected π^0, generate a large number of decays to estimate the contamination.

- Detect the two photons.
- Detect only one of the two photons.
- Considered as exclusive photon events.

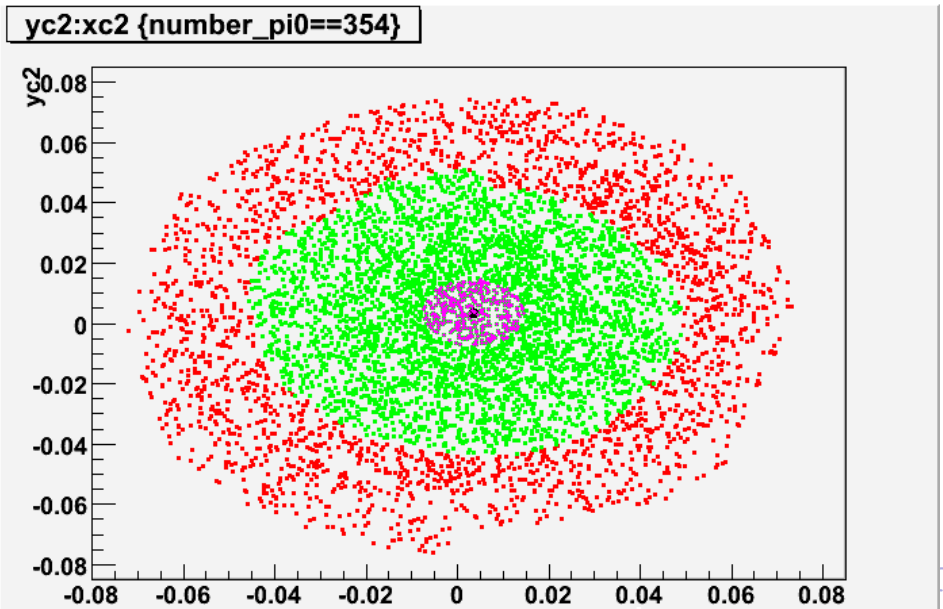

$N_{M_X^2 < M_{cut}^2} = N_{ep \to ep\gamma} + N_{acc} + N_{\pi^0 - 1\gamma} + N_{SIDIS}$

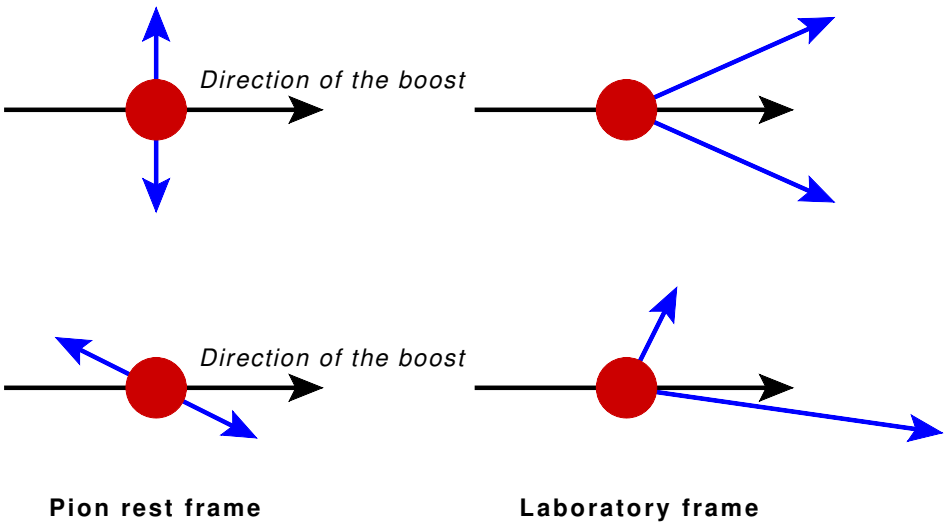

The kinetic energy of the π^0 is shared between the two photons depending on their direction with respect to the π^0 momentum.

We just need to evaluate the phase space of decay contributing to the contamination.

- Advantage: No need for a parameterization of π^0 cross section.
- Drawback: Depends on the ability to detect the 2 photons.

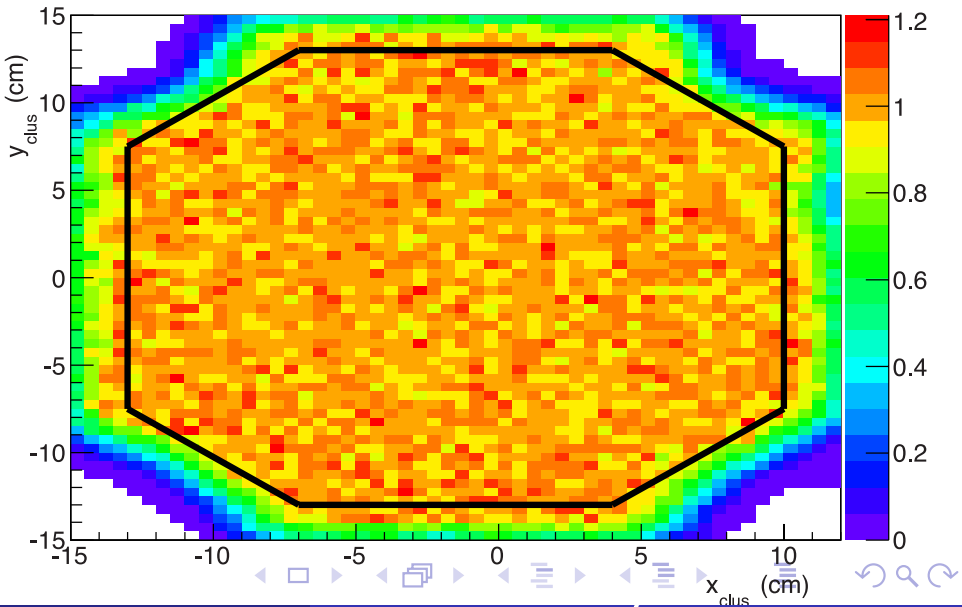

The calorimeter resolution: A crucial effect

The events of a specific t and ϕ bins are located in a specific area of the calorimeter.

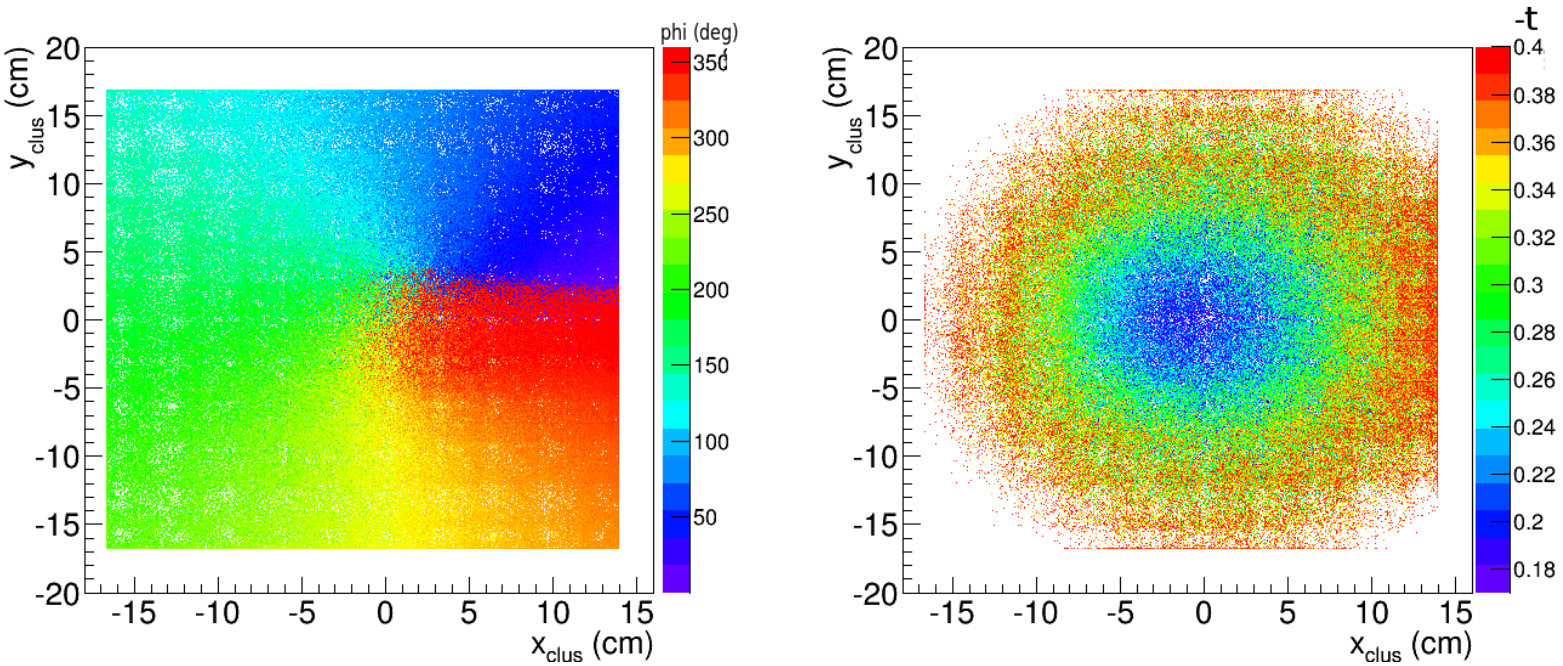

Figure: Left: ϕ-distribution of the events as a function of the photon position in the calorimeter. Right: t-distribution of the events as a function of the photon position in the calorimeter.

The calorimeter resolution: A crucial effect

From one edge of the calorimeter to the other, the energy resolution is not the same ($\phi = 0°$ in red et $\phi = 180°$ in blue).

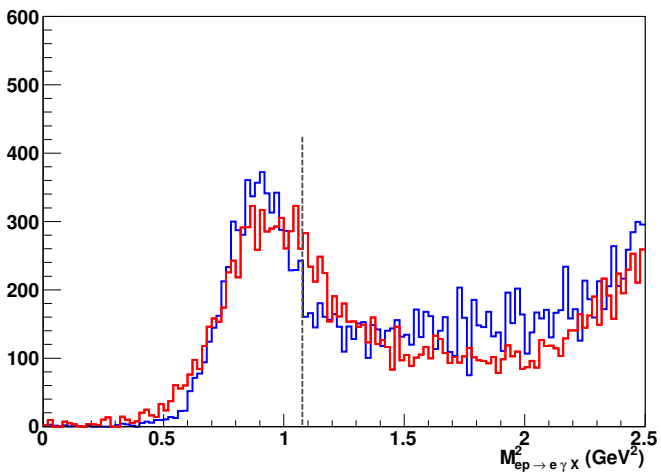

	μ (GeV^2)	σ (GeV^2)
Beam-side (red)	0.964	0.213
180°-side (blue)	0.902	0.144
sum (red+blue)	0.914	0.167

Table: Mean value μ and standard deviation σ of a gaussian fitted on the squared missing mass distributions.

Assuming a uniform resolution and calibration, we would have induced a -15% shift of the cross section at 0° and +5% at 180°.

The calorimeter resolution: A crucial effect

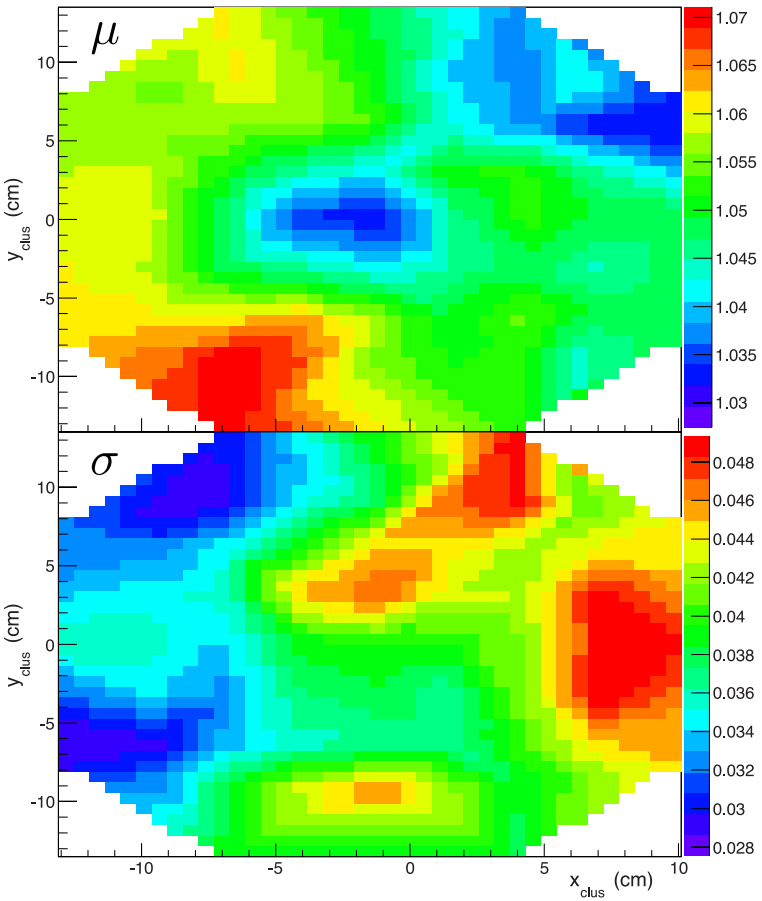

I have developed a calibration/smearing/fit method for the Monte-Carlo calorimeter

$$\begin{pmatrix} q_x \\ q_y \\ q_z \\ E \end{pmatrix} \longmapsto gaus(\mu, \sigma) \times \begin{pmatrix} q_x \\ q_y \\ q_z \\ E \end{pmatrix},$$

which reproduces locally the resolution.